Liliana Reis Damas

Optimization of Lipid Nanoparticle Properties

Dissertação de Mestrado em Tecnologias do Medicamento, orientada pelo

Professor Doutor João José Sousa e apresentada à Faculdade de Farmácia da Universidade de Coimbra

Julho 2013

UNIVERSIDADE DE COIMBRA

TABLE OF CONTENTS

ACKNOWLEDGEMENTS

I wish to thank Prof. Dr. João José Sousa for all his support since I have started as a Master student. His guidance and advice were essential not only for the accomplishment of this work, but also during my graduation, allowing me to grow as a person, student, and professional. I thank him for his immense knowledge, helpful remarks, constant support and motivation. I cannot say thank enough for all the time and efforts he dedicated towards this project, and for his promptitude helping me to overcome the obstacles that arose along the way.

I would like to express my sincere gratitude to Prof. Dr. Alberto Canelas Pais for the opportunity he gave me to work with him. I would like to thank him for sharing his great knowledge about experimental design and the process of optimization, and for his inestimable assistance during my work. I thank him for his encouragement to face the constant difficulties and obstacles of scientific research, and for his promptitude in evaluating and revising my work.

I wish to thank Prof. Dr. Marta Piñeiro for sharing her unique background about photodynamic therapy and porphyrins, and for her scientific advice and insightful suggestions during all the practical and theoretical work. I am deeply thankful for her support and encouragement. Her constant motivation and enthusiasm gave me hope to overcome the major obstacles that emerged during this work.

A special thanks to Dr. Carla Vitorino for her wonderful friendship, support and patience, as well as for sharing her helpful suggestions and points of view, which allowed me to improve my work. I wish to thank her for all the time devoted to help me clarifying all my doubts during this work.

I thank Mrs. Regina and Mr. Pedro for their valuable technical assistance in the laboratory.

I also thank my colleagues from the Pharmaceutical Technology Department, Ana Cláudia Santos, Marlene Lopes, Bárbara, Marisa Gaspar and Raquel Teixeira for all the problems we shared and solved together, and for all the moments of mutual encouragement during this year.

To my dearest friends Ana Penedones, Diogo Oliveira, Tânia Gonçalves, Rita Monteiro and Inês Martins I would like to thank for their great friendship and for understanding every time I deny their company. It is amazing to see the challenges we have come through, and

how much we have grown since the first time we meet. Thanks for accompanying me in the good and bad times!

To my parents I would like to thank for their endless love, understanding and supporting my choices, during all my life. None of this would be possible without them!

A special thanks to Hugo, for the everyday support and encouragement, and for the faith and trust in me. I am deeply thankful for all the love and patience he gave me during this year. Thank you for always pulling me up!

ABSTRACT

Photodynamic therapy has emerged as an important therapeutic option for the treatment of localized cancers. Although the development of new photosensitizers, such as porphyrins and porphyrins derivatives, brought important improvements to this field, the clinical use of photodynamic therapy is still restricted due to various issues. One of the most important problems to overcome in photodynamic therapy is drug delivery. Research for new delivery methods, formulations and targeting strategies have been conducted, and nanoparticles represent emerging photosensitizer carriers. In particular, solid lipid nanoparticles and nanostructured lipid carriers have been little exploited for incorporation of photosensitizers, but have proven their advantages such as low toxicity, good *in vivo* tolerance, and high drug loading. To achieve a formulation with the desired properties, it is important to assess how the system is influenced by several factors. Experimental design has been applied in this field with success. Thus, the aim of this work was the optimization of nanoparticle properties (SLN and NLC) applying experimental design in order to achieve a system capable of incorporation of photosensitizers. The optimization process leaned on the formulation composition. Several factors were evaluated, such as lipid concentration, emulsifier concentration, the absence or present of a liquid lipid, and the liquid:solid lipid ratio, and different components were also studied, in order to achieve a formulation with small particle size and adequate stability. After, various porphyrins were selected for incorporation on the optimized system to confirm its application.

RESUMO

A terapia fotodinâmica tem emergido como uma opção terapêutica importante no tratamento de cancros localizados. Apesar do desenvolvimento de novos fotossensibilizantes, como por exemplo as porfirinas e derivados de porfirinas, possibilitar uma melhoria considerável nesta área, a aplicação clínica da terapia fotodinâmica é ainda limitada devido a várias questões. Um dos problemas mais importantes na terapia fotodinâmica é a administração localizada do fármaco (*drug delivery*). Têm sido estudados vários sistemas para administração localizada do fármaco e estratégias de direccionamento, sendo que as nanopartículas apresentam grande potencial como transportadores de fotossensibilizantes. Em particular, as nanopartículas de lipídicas sólidas (*solid lipid nanoparticles*, SLN) e transportadores lipídicos nanoestruturados (*nanostructured lipid carriers*, NLC) têm sido pouco exploradas para incorporação de fotossensibilizantes, mas demonstraram já as suas vantagens, tais como baixa toxicidade, boa tolerância *in vivo* e a elevada capacidade de incorporação do fármaco. Para obter uma formulação com as propriedades desejadas, é importante para avaliar a forma como o sistema é influenciado por vários factores. Aqui, o *design* experimental tem sido aplicado com sucesso. Assim, o objetivo deste trabalho foi a otimização das propriedades de nanopartículas lipídicas (SLN e NLC) aplicando um *design* experimental, de modo a obter um sistema capaz de incorporar fotossensibilizantes. O processo de otimização baseou-se na composição da formulação. Vários factores foram avaliados, tal como a concentração de lípido, a concentração de tensioactivo, a ausência ou presença de um lípido líquido, a proporção lípido sólido:líquido, e diferentes componentes da formulação, a fim de obter uma formulação com tamanho de partícula reduzido e estabilidade adequada. Posteriormente, várias porfirinas foram seleccionadas para incorporação no sistema otimizado, de modo a confirmar a sua aplicação.

LIST OF FIGURES

LIST OF TABLES

LIST OF ABBREVIATIONS

AFM	atomic force microscopy
ALA	5-aminolevulinic acid
ATR-FTIR	attenuated total reflectance infrared spectroscopy
B60	5,10,15,20-*tetrakis*(4-carboxyphenyl)porphyrin
DSC	differential scanning calorimetry
EE	entrapment efficiency
EPR	enhanced permeability and retention effect
ESR	electron spin resonance
FR	folate receptor
HpD	hematoporphyrin derivative
HPH	high pressure homogenization
HPPH	2-devinyl-2-(1-hexyloxyethyl) pyropheophorbide
LD	laser diffractometry
MP-1046	5,15-*bis*(3-hidroxiphenyl)porphyrin
NLC	nanostructured lipid carriers
NMR	nuclear magnetic resonance
PCS	photon correlation spectroscopy
PDT	photodynamic therapy
PEG	polyethylene glycol
PI	polydispersity index
PIDS	polarization intensity differential scattering
PLA	*poly*(*D,L*-lactide)
PLGA	*poly*(*D,L*-lactide-co-glycolide)
PS	photosensitizer
p-THPP	*meso*-tetra(hydroxyphenyl)porphyrin
RES	reticuloendothelial system
ROS	reactive oxygen species

SD	standard deviation
SEM	scanning electronic microscopy
SLN	solid lipid nanoparticles
TEM	transmission electron microscopy
TPP	5,10,15,20-tetraphenylporphyrin
UV	ultraviolet

Chapter 1

Introduction and Objectives

1. Introduction and Objectives

The aim of the present thesis was the optimization of lipid nanoparticles properties, in particularly solid lipid nanoparticles (SLN) and nanostructured lipid carriers (NLC), and the investigation of the potential of these as carriers systems for porphyrins for application on photodynamic therapy.

The present dissertation has been divided in 8 chapters. In Chapter 2, an introduction on photodynamic therapy and its mechanisms is provided. Moreover, the application of porphyrins as potential photosensitizers in photodynamic therapy is referred. Chapter 3 presents several delivery systems and some successful application of the same. Emphasis is given to SLN and NLC, since these were the systems chosen for optimization.

Chapter 4 contains an introduction to Experimental Design. A definition of experimental design is given, and several experimental designs are described in detail, since it is the main theme of the present thesis. The importance of the application of an optimization process is also mentioned.

In Chapter 5, all the materials and methods used to execute the present work are described in detail.

Chapter 6 presents the results obtained from the optimization process and the respective discussion. The results pertaining to the incorporation of the porphyrin in the optimized formulation are presented in Chapter 7.

Some final remarks on the investigation performed, and some perspectives to future work are included in Chapter 8.

CHAPTER 2
PHOTODYNAMIC THERAPY

2.1. A HISTORICAL PERSPECTIVE ON PHOTODYNAMIC THERAPY

The medical application of photodynamic therapy (PDT) was first described by von Tappeiner and Jesionek in 1903, who used the combination of light and topically applied eosin to treat basal cell carcinomas (BONNETT, 2000). Later, von Tappeiner and Jesionek defined PDT as the dynamic interaction among light, a photosensitizing agent, and oxygen resulting in tissue destruction (DOLMANS, 2003; TRIESSCHEIJN *et al.*, 2006). The first study with PDT in humans was performed in 1913 by Friedrich Meyer-Betz, who injected himself intravenously with hematoporphyrin, and experienced a prickling and burning sensation after exposing himself to sunlight. However, it took decades until PDT breakthrough as a possibility for the treatment of cancer. In the 1960s, Lipson and E.J. Baldes studied a hematoporphyrin derivative (HpD), and concluded that it was a powerful photosensitizer. This localized preferentially in tumor tissue, where emitted fluorescence (LIPSON and BALDES, 1960; LIPSON, BALDES, and OLSEN, 1961; BONNETT, 2000; DOLMANS, 2003).

Later in 1975, Dougherty reported that HpD in combination with red light could completely erradicate mouse mammary tumor growth (DOUGHERTY *et al.*, 1975; DOLMANS, 2003; TRIESSCHEIJN *et al.*, 2006). Three years later, Dougherty reported the first successful treatment of several patients with PDT (DOUGHERTY *et al.*, 1978).

During the next years, further clinical trials were initiated concerning a variety of cancers and photosensitizers, resulting on the regulatory approval of Photofrin® (porfimer sodium) in Canada, in 1993, for the treatment of bladder cancer. Currently, more sensitizers based on natural occurring porphyrins and chlorins are approved for clinical use: 5-aminolevulinic acid, which is a natural precursor of protoporphyrin IX (ALA, Levulan®; DUSA Pharmaceuticals Inc., Wilmington, MA), the methyl ester of ALA (Metvix®; Photocure ASA, Oslo, Norway), and *meso*-tetra-hydroxyphenyl-chlorin (mTHPC, temoporfin, Foscan®; Biolitec Pharma Ltd., Dublin, Ireland). These and other photodynamic drugs that have been approved are presented on Table 1. With these developments, PDT has emerged as an important therapeutic option for the treatment of localized cancers (TRIESSCHEIJN *et al.*, 2006; SERRA *et al.*, 2008).

Table 1. Therapeutical applications for approved photosensitizers (Adapted from TRIESSCHEIJN *et al.*, 2006; SERRA *et al.*, 2008).

Photosensitizer	**Comercial Name**	**Cancer Type**
Polyhematoporphyrin ether/ester	Photofrin®	Cervical cancer
	Photogem®	Endobronchial cancer
	Photosan®	Bladder cancer
	Hematoporphyrin Injection®	Esophageal cancer
		Gastric cancer
meso-tetra-hydroxyphenyl-chlorin	Foscan®	Head and neck cancer
		Additional indications for prostate and pancreatic tumors
5-aminolevulinic acid (ALA)	Levulan®	Actinic keratosis
		Basal cell carcinoma
5-aminolevulinic acid methyl ester	Metvix®	Basal cell carcinoma
		Actinic keratosis
Mono-***L***-aspartyl-chlorin e6	Laserphyrin®	Lung Cancer
	Talaporfin Sodium®	
Benzoporphyrin derivative monoacid ring A	Verteporfin or Visudyne®	Basal cell carcinoma
Sulphonated Aluminium Phthalocynanine	Photosense®	Lung cancer
		Head and neck cancer

2.2. MECHANISM OF PHOTODYNAMIC THERAPY

PDT requires three elements: a photosensitizer (PS), light and oxygen. After the administration of a PS (orally, topically, or intravenously), the tumor tissue is locally illuminated with light of the appropriate wavelength, at an appropriate time after administration corresponding to a maximum PS accumulation in tumor tissue, to activate the sensitizer. Following absorption of light, the PS, initially at a ground state (^{0}PS), transforms into a short-lived excited state (^{1}PS*) that may convert into a long-lived triplet state (^{3}PS*). In the photosensitization process, the singlet state is a precursor of the triplet state (Figure 1).

This may generate cytotoxic species by undergoing two main reactions. In the presence of oxygen, it can react directly with oxygen molecules or other substrate molecules by proton or electron transfer, resulting in the formation of free radicals or radical ions which can react with molecular oxygen to produce oxygenated products (Type I reaction). Alternatively, the energy of the triplet state can be directly transferred to oxygen, producing singlet oxygen (Type II reaction). Singlet oxygen is the most damaging species generated during PDT (KONAN, GURNY, and ALLÉMANN, 2002; LUKŠIENE, 2003; DOLMANS, 2003; TRIESSCHEIJN *et al.*, 2006; BECHET *et al.*, 2008; CHATTERJEE, FONG, and ZHANG, 2008).

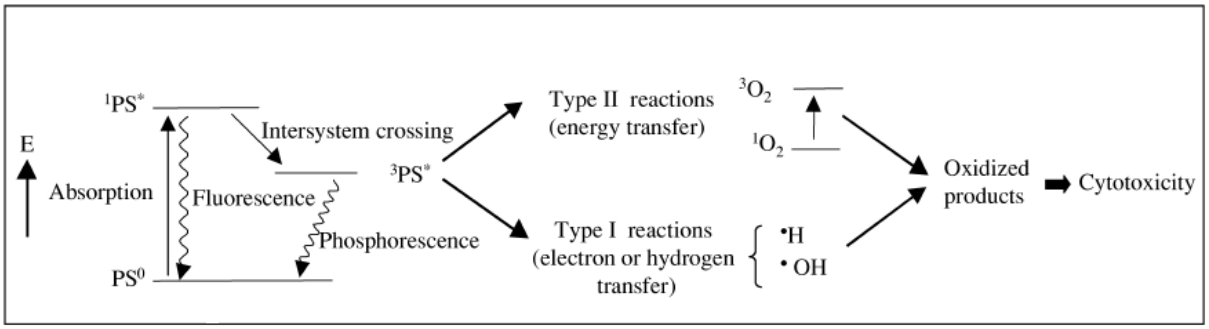

Figure 1. Mechanism of PDT cytotoxicity; photophysic reactions represented by modified Jablonski diagram (Adapted from KONAN, GURNY, and ALLÉMANN, 2002).

There are three main pathways by which PDT mediates tumor destruction. As mentioned, reactive oxygen species (ROS) have a main role in the photosensitization process, with the ability to kill tumor cells directly. PDT can also damage the tumor vasculature, or it can activate an immune response against the tumor cells (LUKŠIENE, 2003; DOLMANS, 2003).

The PDT efficiency depends on several factors such as the PS chemical properties, the pharmaceutical formulation in which it is incorporated, the amount of PS in treated tissue, the time of activation with light, the light doses and the amount of oxygen available (KONAN, GURNY, and ALLÉMANN, 2002; LUKŠIENE, 2003; TRIESSCHEIJN *et al.*, 2006).

2.3. PHOTOSENSITIZERS

Since the photosensitizer is a critical element in PDT, a large number of photosensitizing drugs have been tested *in vitro* and *in vivo* during the last years (LUKŠIENE, 2003). The ideal PS should be a chemically pure drug with the ability to selectively accumulate in the tumor tissue, with a rapid clearance, a strong absorption peak at light wavelength beyond 630 nm,

minimum dark toxicity and maximum cytotoxicity in the presence of light, and would have a high quantum yield and long lifetime of triplet state (TRIESSCHEIJN *et al.*, 2006).

First generation photosensitizers are hematoporphyrin, its derivative (HpD), and the purified, commercially available Photofrin® (porfimer sodium). Today, Photofrin® is currently approved by the US Food and Drug Administration for treatment of esophageal cancer, endobronchial cancer and high-grade dysplasia in Barrett's Esophagus (PINNACLE, 2011). However, these first generation photosensitizers suffered from several limitations as poor selectivity, need for large amounts of drug to obtain good efficiency, and high cutaneous photosensitivity, limiting their clinical applications (CHATTERJEE, FONG, and ZHANG, 2008). Significant tissue penetration is achieved by light at 630 to 635 nm, which corresponds to the weakest absorption of Photofrin® (LUKŠIENE, 2003). These problems lead to the development of new molecules, the second generation PS, including porphyrin derivatives, phthalocyanines, naphthalocyanines and chlorins (HOPPER, 2000; KONAN, GURNY, and ALLÉMANN, 2002). These are pure and well-characterized compounds. They are effective generators of singlet oxygen, and have a strong absorption peak in the wavelength range of 650-800 nm, wavelength at which light penetration in tissue is higher. Better tumor selectivity and relatively fast elimination, leading to shorter periods of photosensitivity, are other advantages of the second generation of photosensitizers (HOPPER, 2000; KONAN, GURNY, and ALLÉMANN, 2002; CHATTERJEE, FONG, and ZHANG, 2008). Yet, most of these PS molecules are hydrophobic and can aggregate easily in aqueous environment. This is a key factor, since the sensitizer molecules preferentially accumulate in the lipophilic compartments of tumor cells, including plasma, mitochondrial, endoplasmic reticulum, nuclear and lysosomal membranes (KONAN, GURNY, and ALLÉMANN, 2002; LUKŠIENE, 2003; PASZKO *et al.*, 2011). Moreover, the selective accumulation of the PS in tumor tissue is required to avoid collateral damage to healthy tissue. Thus, it became important to develop delivery systems capable of protecting the PS from the aqueous environment. The third generation PS comprises suitable delivery systems (oil dispersions, liposomes, polymeric nanoparticles) and the use of PS complexed with serum lipoproteins or conjugated with specific monoclonal antibodies, in order to enhance the uptake by targeted tissue, improving PDT efficiency (KONAN, GURNY, and ALLÉMANN, 2002).

2.4. SINGLET OXYGEN

Molecular oxygen is one of the most important substances on the earth, and is crucial in the photosensitization process. The two electronically excited states immediately above the

ground state are both singlet states, namely $^1\sum_g^+$ and $^1\Delta_g$. The first one is very short-lived, and rapidly decays to the lower singlet state, designated $^1\Delta_g$ or $^1O_2$, which has a lifetime of a few microseconds in the condensed phase. The lifetime of singlet oxygen in solution varies with the solvent, but generally it is below 3.5 μs and can diffuse only 0.01 to 0.02 μm during this period (BONNETT, 2000; HOPPER, 2000; CHATTERJEE, FONG, and ZHANG, 2008). Thus, the initial extent of the damage is limited to the site of concentration of the PS molecule, which is usually the mitochondria, plasma membrane, golgi apparatus, lysosomes, endosomes and endoplasmic reticulum.

A key property of a PS is the quantum yield of singlet oxygen (Φ_Δ) which is defined as

$$\Phi_\Delta = \frac{\text{The number of } ^1O_2 \text{ generated}}{\text{The number of photons absorbed}}$$

There are several techniques described for the detection and measurement the quantum yield of singlet oxygen. These include indirect methods, such as the use of a target substrate and the observation of its degradation caused by singlet oxygen, or the measurement of singlet oxygen decay, by phosphorescence detection (WILKINSON, HELMAN, and ROSS, 1993).

2.5. Porphyrins as Potential Photosensitizers

Porphyrins are present in natural systems, making them ideal candidates for use in biological singlet oxygen generation. Their low toxicity in the dark, and ability to absorb several wavelengths in the UV-visible range led to several studies of their uses as PS in PDT. Porphyrins and porphyrin-related macrocycles are among the sensitizers most frequently used in PDT. They are aromatic macrocycles that exhibit characteristic optical spectra with a very strong band at 400 nm, called Soret or B band, and usually four distinct bands in the visible region, called Q bands (BONNETT, 2000). The long-lived triplet states of many porphyrins allow for high quantum yields. Tuning of photophysical effects can be achieved through the modification at the periphery of the macrocycle, coordination of metal ions at its center, and ligands attached to the axial positions of the metal ion. Its rapid decomposition in the presence of singlet oxygen (photobleaching) could be an advantage in biological systems where rapid breakdown of the PS after use is necessary. The modification of readily available porphyrins, hematoporphyrin and protoporphyrin, was an obvious first step in the search for new PS (DEROSA and CRUTCHLEY, 2002; DABROWSKI *et al.*, 2007).

2.6. Future Directions in Photodynamic Therapy

Besides the important improvement brought by the new generation of PS, the clinical use of PDT is still limited due to several issues. As mentioned before, there are many properties that determine the effectiveness of this method such as the singlet oxygen production and the degree of selectivity to the target tissue. Regardless of the clinically approved PS, there is not an ideal, safe and selective one, which allows low photosensitization and minor secondary effects. Several approaches can be taken in order to achieve a selective accumulation of the PS in tumor tissue and to increase the solubility of hydrophobic PS, enhancing PDT efficacy. There are other aspects that can be improved such as light dosimetry and production of singlet oxygen. Still, one of the most important problems to overcome in PDT is drug delivery. In this regard, research for new delivery methods, formulations and targeting strategies have been conducted (PASZKO *et al.*, 2011). Nanoparticles represent emerging PS carriers that show great promise for PDT (BECHET *et al.*, 2008). Nanoparticles can increase the solubility of hydrophobic drugs, and its hydrophilicity and proper size, allows accumulation in tumor tissue, based on the enhanced permeability and retention effect (EPR). Moreover, by modifying the surface area using other ligands, selective accumulation can be enhanced. This represents an attractive strategy to increase drug delivery to cancer cells, thus avoiding collateral damage to healthy tissue (BECHET *et al.*, 2008; PASZKO *et al.*, 2011). The ideally delivery system should be biodegradable, have a small size and high loading capacity, minimal internal toxicity, ability to incorporate the PS without loss or alteration of its activity, protecting the PS from enzymatic or biological degradation, minimal self-aggregation tendency and should selectively accumulate in required area in therapeutic concentration with little or even no uptake by non-target cells (KONAN, GURNY, and ALLÉMANN, 2002; BECHET *et al.*, 2008; PASZKO *et al.*, 2011; LIM *et al.*, 2012). Further discussion on this topic will be presented in Chapter 3.

CHAPTER 3

NANOCARRIERS FOR PHOTODYNAMIC THERAPY

Interest in nanoparticles as drug carriers has been increasing due to their ability to transport hydrophobic drugs in blood and their large surface area which allows modifications with functional groups, improving nanoparticles chemical/biological properties. Moreover, they have large distribution volumes, and are generally taken up efficiently by cells (CHATTERJEE, FONG, and ZHANG, 2008). Nanocarriers may provide more effective or convenient routes of administration, lower therapeutic toxicity and extend drug release characteristics and immunogenicity. As therapeutic delivery systems, nanoparticles allow targeted delivery and controlled release. These have been studied for application on several administration routes. As an example, for parenteral administration, particular attention should be given to particle size. Large particles increase the risk of embolism. The mean particle size is usually around 200–500 nm, and there are strict limitations concerning the presence of microparticles (BUNJES, 2010).

Due to their small size, nanoparticles are capable of accumulating in pathological areas, as solid tumors and infarcted areas, via the enhanced permeability and retention effect (EPR) (KONAN, GURNY, and ALLÉMANN, 2002; TORCHILIN, 2007; PASZKO *et al.*, 2011). Unlike in normal tissue, the vasculature in pathological areas is penetrable for large and small particles allowing their extravasation and accumulation in an interstitial tumor tissue. This is facilitated also by the pore size in tumors, which varies from 200 nm to 600 nm, and by the poor lymphatic drainage and increased vessel permeability. A major drawback of nanoparticles is their propensity to be taken up by the macrophages after intravenous administration and accumulation in the spleen and the liver, thus reducing the circulation time of nanoparticles. Coating of nanoparticles is a strategy frequently used to avoid the reticuloendothelial system (RES) uptake. The most widely used polymeric steric stabilizer is polyethylene glycol (PEG) (CHEN, POGUE, and HASAN, 2005; TORCHILIN, 2007; CHATTERJEE, FONG, and ZHANG, 2008; PASZKO *et al.*, 2011).

Several strategies have been developed to encapsulate PS into nanoparticles and also improve delivery to the target tissue. As most PS are hydrophobic, liposomes, polymeric nanoparticles, micelles, ceramic based nanoparticles, gold nanoparticles, and others, have been considered to protect the PS from the aqueous environment. In addition to an increase in drug delivery, photochemical internalization, i.e., the light triggered release of the active drug into the cytosol can also offer potential improvements (KONAN, GURNY, and ALLÉMANN, 2002; CHATTERJEE, FONG, and ZHANG, 2008; PASZKO *et al.*, 2011).

In 2002, Konan *et al.* published a comprehensive review on delivery of PS in PDT. Here, the authors divided the processes into passive and active, based on the presence or absence of a targeting molecule in the surface. A delivery system that incorporates target tissue receptors or antigens to deliver the PS specifically to diseased tissue, was named as "active targeting system", while other formulations that enable parenteral administration and passive targeting where termed "passive targeting systems" (KONAN, GURNY, and ALLÉMANN, 2002). Nevertheless, nanoparticles often themselves are photoactive or have an additional intermediary role in the overall process (CHATTERJEE, FONG, and ZHANG, 2008; PASZKO *et al.*, 2011).

3.1. LIPOSOMES

Liposomal carriers are often studied as drug carriers, due to their simple structure, controllable size, and convenient preparation procedure. However, liposomes have short plasma half-lives, which is insufficient for tumor cell uptake given the rapid elimination by the RES and decomposition due to lipid exchange from molecular interaction with liposome components. Liposomes with uni- or multi-lamellar lipid bilayers show proper retention of drugs and good and rapid accumulation and release characteristics in tumor cells. According to the physical properties of PSs, liposomes can be optimized. Smaller liposomes have a more efficient accumulation and retention and, thus, size control in conjunction with PS is an important feature in the use of liposomal carriers. With the aim of prolonging the circulation in bloodstream and improving structural stability, specifically modified liposomes have been developed by modifying surface properties. Hence, a higher concentration of liposomes can accumulate in the tumor, resulting in an increase in the delivery amount of available PSs (BOVIS *et al.*, 2012; LIM *et al.*, 2012).

3.2. POLYMERIC NANOPARTICLES

Polymeric nanoparticles emerge as more attractive delivery systems owing their high stability and small/uniform particle size distribution, which contributes to their passive targeting delivery via EPR effect, and prevents recognition by macrophages and proteins, extending circulation time in the blood (LIM *et al.*, 2012). The chemical composition and architecture of polymers can be designed to accommodate drugs with different degrees of hydrophobicity, molecular weight and charge. The surface properties, morphologies, and composition of polymer matrices can be easily optimized for controlled drug polymer degradation and drug release kinetics for controlled release of the PS (CHATTERJEE, FONG, and ZHANG, 2008). Usually, photosensitizers are confined between the drug and

the polymer by hydrophobic or electrostatic interactions. By altering the polymer composition, the size of polymeric nanoparticles can be controlled for optimize transport into tumor cells. However, polymeric nanoparticles have a high tendency to be taken up by the RES after intravenous administration and accumulation in the spleen and in the liver, which represents a major drawback (LIM *et al.*, 2012).

Due to versatility, physical robusteness, biocompatibility, high drug loading efficiency and controlled drug release, polyglicolide (PGA), polyactide (PLA), and their copolymer *poly*(*D,L*-lactide-co-glycolide) (PLGA) have been mostly used in polymeric nanoparticles.

In 2002, Konan *et al*, encapsulated *meso*-tetra(hydroxyphenyl)porphyrin (*p*-THPP) into sub-130 nm biodegradable nanoparticles using three selected polyesters (*poly*(*D,L*-lactide-co-glycolide), (50:50 PLGA, 75:25 PLGA) and *poly*(*D,L*-lactide (PLA)) by emulsification-diffusion, with drug loadings of up to 7% (w/w) (KONAN, CERNY, *et al.*, 2003; KONAN, BERTON, *et al.*, 2003). The study performed to evaluate the photodynamic activity of *p*-THPP loaded nanoparticles on EMT-6 mouse mammary tumor cells as compared to free *p*-THPP revealed that cell viability was drug concentration-dependent, and the encapsulation of *p*-THPP improved its therapeutic index, since low drug concentrations could be used for satisfactory photocytotoxicity. Furthermore, the use of small drug concentrations could be a means of minimizing the undesirable effects. It was also reported that the polymer nature could affect the photocytotoxic efficiency of *p*-THPP incorporated into nanoparticles. In summary, the relatively low drug concentration and the short incubation times of nanoparticles with cells required to induce satisfactory photodynamic damages demonstrated that *p*-THPP loaded nanoparticles offer superior photoactivity as compared to the free drug (KONAN, BERTON, *et al.*, 2003).

3.3. Ceramic-based Nanoparticles

Ceramic-based nanoparticles hold numerous advantages over organic polymeric nanoparticles. These particles can be produced with the desired size, shape and porosity, and the process for the production requires simple ambient temperature conditions. Their low size, less than 50 nm, is an important feature allowing these to evade capture by the RES. In addition, ceramic based nanoparticles have immunity to changes in pH and microbial attack. Ceramic nanoparticles are highly stable, and may not release the entrapped drugs, even at extreme conditions of pH and temperature. Yet, their porous matrix is permeable to molecular as well as singlet oxygen, and thus the photodestructive effect will be maintained in the encapsulated form. The encapsulation of an effective PS (2-devinyl-2-(1-

hexyloxyethyl) pyropheophorbide (HPPH)) in ceramic-based nanoparticles revealed the potential of these nanoparticles. Irradiation of the photosensitizing drug entrapped in the nanoparticles with light of suitable wavelength resulted in an efficient generation of singlet oxygen, which is made possible by the inherent porosity of the nanoparticles. The HPPH-loaded nanoparticles were actively taken up by cultured UCI-107 and HeLa tumor cells. Irradiation at 650 nm with a laser caused significant tumor cell death, leaving less than 10% of HeLa cells viable (ROY *et al.*, 2003; CHATTERJEE, FONG, and ZHANG, 2008).

3.4. GOLD NANOPARTICLES

In 2006, Wieder *et al.* developed a delivery system based on gold nanoparticles, whereby the PS is bound to the surface of the nanoparticle. The PS used was a phthalocyanine derivative. The produced phthalocyanine-nanoparticle conjugates had an average diameter of 2–4 nm. After irradiation of the internalized phthalocyanine-nanoparticle conjugates, a decrease in cell viability to 43% was observed in comparison to the free phthalocyanine. The 50% enhancement of singlet oxygen quantum yields observed for the phthalocyanine-nanoparticle conjugates lead to this significant improvement in PDT efficiency. These results show the great potential that gold nanoparticles conjugates have as a delivery system for photosensitizers in PDT (WIEDER *et al.*, 2006; CHATTERJEE, FONG, and ZHANG, 2008).

3.5. SOLID LIPID NANOPARTICLES (SLN)

In the beginning of the 90s, solid lipid nanoparticles (SLN) were developed as an alternative to traditional carrier systems such as emulsions, liposomes and polymeric nanoparticles (SOUTO, 2003). SLN consists of a lipid solid at room temperature but also at body temperature (MÜLLER, RADTKE, and WISSING, 2002) which is stabilized by an emulsifier. They have a size range in between 50 and 1000 nm (MÜLLER, MÄDER, and GOHLA, 2000). SLN combined the advantages of other innovative carrier systems such as physical stability, protection of the incorporated drug from degradation, controlled drug release, good tolerability, and minimized the problems associated with them (WISSING, KAYSER, and MÜLLER, 2004). A clear advantage of SLN is the fact that the lipid matrix is made from physiological lipids, providing a low toxicity and good *in vivo* tolerance. The choice of the emulsifier depends on the administration route, and is more limited for parenteral administration, since here the emulsifier has a key role in the interaction with cells (MEHNERT and MÄDER, 2001; MÜLLER, SHEGOKAR, and KECK, 2011). Different solid lipids and emulsifiers have been used, as shown in Table 2. Some disadvantages of this system are the insufficient loading capacity and drug expulsion during storage. The drug

loading capacity is limited by the solubility of drug in the melted lipid, the structure of lipid matrix and the polymorphic state of the lipid matrix. The drug expulsion during storage is caused by transition to highly ordered lipid particles. After production, lipids crystallize in high energy modifications (α, β') with more imperfections in the crystal lattice. During storage, if a transition to form β takes place, the drug will be expelled from the lipid matrix (WISSING, KAYSER, and MÜLLER, 2004).

Table 2. Lipids and emulsifiers used for the preparations of lipid nanoparticles (Adapted from MEHNERT and MÄDER, 2001; PUGLIA and BONINA, 2012).

Lipids	Tripalmitin
	Glyceryl behenate (Compritol® 888 ATO)
	Glyceryl palmitostearate (Precirol® ATO 5)
	Stearic acid
	Oleic acid
	Caprylic/Capric Triglyceride (Miglyol® 812)
	Squalene
Emulsifiers	Poloxamer 188 (Lutrol® F68, Pluronic® F68)
	Polysorbate 80 (Tween® 80)
	Polysorbate 20 (Tween® 20)
	Sodium cholate
	Phosphatidylcholine (Epikuron® 200, Phospholipon® 80/H)
	Soybean lecithin (Lipoid® S75)

This delivery system has been little exploited for the delivery of PS. In 2004, Stevens *et al* evaluated a folate receptor(FR)-targeted SLN as a carrier for a lipophilic derivative of the photosensitizer hematoporphyrin (HpD). The targeted SLN produced had a mean diameter lower than 200 nm, and showed an increased cytotoxicity, from 5.17 to 1.57 μM. Fluorescence microscopy results confirm the selectivity of the FR-targeted SLN (STEVENS, SEKIDO, and LEE, 2004).

3.6. NANOSTRUCTURED LIPID CARRIERS (NLC)

SLN were the first generation of lipid nanoparticle carriers. These systems were considered of high relevance for administration through different pathways, but there was

room for some improvements. The second generation of lipid nanoparticles, the nanostructured lipid carries (NLC), minimizes some potential problems associated with SLN (MÜLLER, RADTKE, and WISSING, 2002).

Basically, the matrix in NLC is composed of a blend of a solid and liquid lipid, which is solid at body temperature. The idea is that by imparting the lipid matrix a certain nanostructure, the pay-load for active compounds is increased and expulsion of the drug during storage is avoided (MÜLLER, RADTKE, and WISSING, 2002). The advantages of including small amounts of liquid lipid into a solid lipid matrix are also related to the possibility of entrapping drugs which are better solubilized in liquid lipids, followed by a higher loading capacity achieved in NLC in comparison to SLN (DOKTOROVOVA and SOUTO, 2009).

In the present work these two delivery systems were investigated for the incorporation of PSs, and a previous detailed study was done aiming at a better understanding of these carriers.

3.7. Preparation Methods of SLN and NLC

There are different methods for preparation of SLN and NLC described in literature (MEHNERT and MÄDER, 2001; MÜLLER, RADTKE, and WISSING, 2002). The most commonly applied are the high pressure homogenization, the microemulsions based SLN preparations and the solvent emulsification/evaporation.

3.7.1. High Pressure Homogenization

High pressure homogenization (HPH) represents the main and most well-known method for produce lipid nanoparticles (PUGLIA and BONINA, 2012). HPH has several advantages compared to other methods, including easy scale up, avoidance of organic solvents and short production time (PARDEIKE, HOMMOSS, and MÜLLER, 2009). This technology also allows the production of nanoparticles with a relatively homogeneous size distribution, which increases the physical stability of the aqueous dispersion (SOUTO, 2003).

High pressure homogenizers push the liquid with high pressure through a narrow gap, and in a very short distance, the fluid accelerates to very high velocity. The cavitation forces and high shear decrease the particle size down to the submicron range (WISSING, KAYSER, and MÜLLER, 2004).

Lipid nanoparticles can be produced by the hot or the cold homogenization technique. In both techniques, the drug is solubilized in the lipid being melted at approximately 5-10°C above its melting point.

3.7.1.1. HOT HIGH PRESSURE HOMOGENIZATION

The melted lipid containing the drug is dispersed in a hot emulsifier solution by high speed stirring. The obtained pre-emulsion is passed through a high pressure homogenizer, at the same temperature. Usually, the production conditions are 500 bar and two or three homogenization cycles (MÜLLER, RADTKE, and WISSING, 2002). The produced nanoemulsion is cooled down at room temperature or at temperatures below, and lipid crystallization leads to the formation of lipid nanoparticles.

High temperatures may increase the degradation rate of the drug, and carrier. Yet, the use of high temperatures results in lower particle sizes due to decreased viscosity of the inner phase (MEHNERT and MÄDER, 2001). A good temperature control is required, since HPH also increases the sample temperature.

Hot HPH is the most frequently applied technique. It can be applied to the entrapment of lipophilic and insoluble drugs, and even temperature sensitive compounds can be processed, since the exposure time to high temperatures is rather short (MÜLLER, RADTKE, and WISSING, 2002).

3.7.1.2. COLD HIGH PRESSURE HOMOGENIZATION

In the cold HPH technique, the drug containing lipid is rapidly cooled by means of dry ice or liquid nitrogen, grounding the solid lipid to lipid microparticles. The high cooling rate favors a homogenous distribution of the drug within the lipid matrix (MEHNERT and MÄDER, 2001). The microparticles are then dispersed in a cold emulsifier solution by high speed stirring. The formed suspension is passed through a high pressure homogenizer, at or below room temperature, where the cavitation forces break the lipid microparticles directly to solid lipid nanoparticles (MÜLLER, MÄDER, and GOHLA, 2000).

It should be kept in mind that low temperatures increase fragility of the lipid, and favour, therefore, particle disruption (MEHNERT and MÄDER, 2001).

The cold HPH is recommended for extremely temperature sensitive compounds and hydrophilic compounds, because they would partition between the melted lipid and the water phase during the hot homogenization process (MÜLLER, MÄDER, and GOHLA,

2000). This technique minimizes the melting of the lipid and therefore minimizing loss of hydrophilic drug to the water phase.

3.7.2. Microemulsions Based SLN Preparations

The microemulsion technique developed by Gasco is based on the dilution of microemulsions (MEHNERT and MÄDER, 2001).

Microemulsions are clear solutions composed by a lipophilic phase, an emulsifier, and in most cases also a co-surfactant and water (MÜLLER, MÄDER, and GOHLA, 2000). For the production of SLN by this technique, a warm microemulsion is prepared by stirring, containing the molten lipid and the emulsifier. This is then dispersed under stirring in excess of cold water, leading to a breaking of the microemulsion, converting it into an ultra-fine nanoemulsion which recrystallizes the internal lipid phase, thus forming lipid particles. The dilution with water and the reduction of temperature breaks the emulsion, narrowing the microemulsion region (SOUTO, 2003). Typical volume ratios of microemulsion to cold water are in range of 1:25 to 1:50 (MEHNERT and MÄDER, 2001). To improve particle concentration the excess of water in then removed by ultrafiltration or by lyophilisation (WISSING, KAYSER, and MÜLLER, 2004).

3.7.3. Solvent Emulsification/Evaporation

In the solvent emulsification-evaporation technique, the lipid is dissolved in a water-immiscible organic solvent that is emulsified in an aqueous phase. Upon evaporation of the solvent a nanoparticle dispersion is formed by precipitation of the lipid in the aqueous medium. An important advantage of this technique is the avoidance of heat during the process, making it suitable for incorporation of temperature sensitive compounds. However, the use of organic solvents is the major disadvantage of this process (WISSING, KAYSER, and MÜLLER, 2004).

3.8. Models for Incorporation of Active Compounds

An innovative and successful carrier system should allow a high loading capacity for incorporated drugs as well as long-term incorporation. The drug can be incorporated between fatty acids, between lipid layers or in imperfections. Depending on the drug/lipid ratio and solubility, the drug has different locations in SLN. There are basically three models for the incorporation of drugs into SLN: homogeneous matrix model, drug-enriched shell model and drug-enriched core model. The obtained structure depends on the formulation

composition and of the production conditions, i.e. hot or cold homogenization (MÜLLER, RADTKE, and WISSING, 2002; WISSING, KAYSER, and MÜLLER, 2004).

Figure 2. Models of incorporation of drugs into SLN (Adapted from MÜLLER, RADTKE, and WISSING, 2002).

A homogeneous matrix with molecularily dispersed drug or drug present in amorphous clusters (Figure 2, left) is thought to be mainly obtained when applying the cold HPH and using no emulsifier or no drug-solubilizing emulsifier, and when incorporating very lipophilic drugs in SLN with the hot HPH. In the first method, the bulk lipid contains the dissolved drug in molecularly dispersed form, mechanical breaking by HPH leads to nanoparticles having a homogeneous matrix structure. The same will happen when the oil droplets produced by the hot HPH are being cooled, crystallize and no phase separation between lipid and drug occurs during this cooling process. This homogeneous matrix model is assumed for drugs that can show prolonged release (MÜLLER, RADTKE, and WISSING, 2002; UNER and YENER, 2007).

An outer shell enriched with drug (Figure 2, middle) can be obtained when phase separation occurs during the cooling process from the liquid oil droplet to the formation of SLN when hot HPH is applied. At increased temperature, the drug partitions from the lipid phase to the aqueous phase. During the cooling process, the drug re-partitions into the liquid lipid phase, due to the decreased solubility in the aqueous phase with decreasing temperature. Since the lipid precipitates first, forming an almost compound-free lipid core, this is not accessible to the drug. Thus, this concentrates in the still liquid outer shell of the SLN or on the surface of the particles. Finally, the compound-enriched shell crystallizes. This model is valid for drugs that lead to a very fast release once the drug in the outer shell and on the particle surface is release in the form of a burst. A fast release can be highly desired when application of SLN to the skin should increase drug penetration, especially when using the occlusive effect of SLN at the same time. On the other hand, when the drug precipitates first, the shell will have distinctly less drug, forming a core enriched with the drug (Figure 2,

right). This leads to a membrane controlled release governed by the Fick law of diffusion. This model is formed when the drug concentration is close to its saturation solubility in the lipid (MÜLLER, MÄDER, and GOHLA, 2000; MÜLLER, RADTKE, and WISSING, 2002).

These models represent the ideal types. There can also be mixed types which can be considered as a fourth model. The structure of SLN formed clearly depends on the physicochemical characteristics of the drugs, components of the formulation and the production conditions (MÜLLER, RADTKE, and WISSING, 2002). Nevertheless, these models also have some flaws.

After hot HPH, lipid crystallization leads to the formation of lipid nanoparticles. The solid lipid can crystallize in high energy modifications (α, β') resulting in a crystal matrix with more imperfections for drug accommodation. During storage, these modifications can transform to the low energy and more ordered β modification. This high degree of order reduces the number of imperfections in the crystal matrix consequently leading to drug expulsion. Hence, a less ordered solid lipid matrix is an important pre-requisite for a sufficiently high drug-load. Figure 3 presents the differences between a perfect crystal in SLN in comparison to a structure with imperfections in NLC.

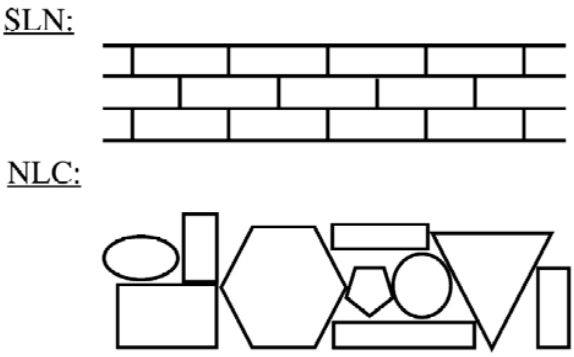

Figure 3. Perfect crystal in SLN comparable with a brick wall (upper) and structure with imperfections due to spacially very different molecules in NLC type I (lower) (Adapted from MÜLLER, RADTKE, and WISSING, 2002).

The formation of a perfect crystal is a potential problem in SLN, as it limits the drug loading, and leads to drug expulsion. However, NLC are produced using spatially different lipids, i.e. blending solid lipids with liquid lipids, resulting in a matrix with enough imperfections to accommodate the drug (Figure 3, lower). There are three types of NLC compared to the more or less highly ordered matrix of SLN (Figure 4).

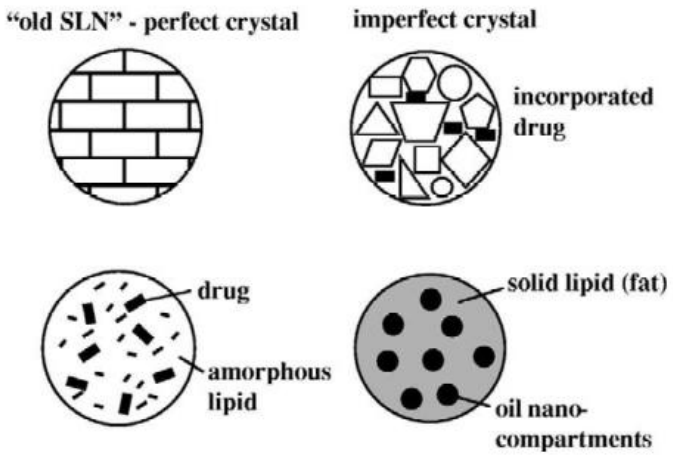

Figure 4. The three types of NLC compared to the relatively ordered matrix of SLN (upper left), NLC types: imperfect type (upper right), amorphous type (lower left), multiple type (lower right) (Adapted from MÜLLER, RADTKE, and WISSING, 2002).

NLC have a lipid matrix which is solid but not crystalline - it is in an amorphous state. This is the "amorphous type" of NLC (Figure 4, lower left). This can be achieved by mixing special lipids, e.g. hydroxyoctacosanylhydroxystearate with isopropylmyristate.

As different lipids are used for the production of NLC, the matrix is highly disordered and has various imperfections to accommodate the drug. NLC based on this principle are called "imperfect crystal type" (Figure 4, upper right).

The third type of NLC is comparable to water/oil/water emulsions. In this case, it is an oil-in-solid lipid-in-water dispersion, where the solid lipid matrix contains small oil nanocompartments (Figure 4, lower right). Solubility of many drugs in a liquid lipid is higher than in a solid lipid. Thus, when lipids lack the appropriate drug solubility, the addition of a higher amount of liquid lipid to the lipophilic phase enables a high solubility for lipophilic drugs, and prevents drug leakage resulting from the exclusive solid matrix (UNER and YENER, 2007). Thus, the development of the "multiple type" of NLC improved the loading capacity for these drugs. These NLC are produced by mixing a solid lipid with higher amount of liquid oil. At low concentrations of oil, the oil molecules are distributed within the solid lipid matrix. When increasing the oil concentration, the solubility of the oil molecules in the solid lipid is exceeded, phase separation occurs and oily nanocompartments are formed. During the cooling-down process, the oil precipitates in the form of fine droplets being incorporated into the solid matrix (MÜLLER, RADTKE, and WISSING, 2002).

Therefore, in comparison to the SLN, it can be said that NLC can be used for all purposes that the SLN are used with additional benefits. NLC possess a higher loading capacity and avoid or minimize drug expulsion during storage due to the less ordered structured of the system.

3.9. Applications of SLN and NLC

Both SNL and NLC have been extensively studied for several administration routes and in cosmetic dermal products (MÜLLER, RADTKE, and WISSING, 2002; WISSING, KAYSER, and MÜLLER, 2004; UNER and YENER, 2007; MÜLLER *et al.*, 2007; PARDEIKE, HOMMOSS, and MÜLLER, 2009; JOSHI and MÜLLER, 2009; MÜLLER, SHEGOKAR, and KECK, 2011).

Lipid nanoparticles received special attention for dermal application in pharmaceutical and cosmetic fields. They provide controlled release for many substances, and the physiological and biodegradable lipids on their composition promote an excellent tolerability. Their small size ensures a close contact to the stratum corneum, and increase the amount of drug penetrated into the skin. Moreover, lipid nanoparticles are able to enhance chemical stability of compounds (MÜLLER *et al.*, 2007; PARDEIKE, HOMMOSS, and MÜLLER, 2009; MÜLLER, SHEGOKAR, and KECK, 2011).

Most of the dermal investigations were done in the cosmetic area. Lipid nanoparticles increased the penetration of actives, such as coenzyme Q10, and skin hydration *in vivo.* The first lipid nanoparticles-based cosmetic product introduced in the market was Cutanova Cream NanoRepair Q10, in 2005. The skin hydration was superior with NLC containing cream in comparison to a conventional o/w cream (PARDEIKE and MÜLLER, 2007; PARDEIKE, HOMMOSS, and MÜLLER, 2009; MÜLLER, SHEGOKAR, and KECK, 2011).

SLN and NLC have been investigated to improve the treatment of skin diseases such as atopic eczema, psoriasis, acne, skin mycosis and inflammations. Celecoxib was investigated for dermal application using NLC-base delivery systems. Celecoxib is widely used for treatment of rheumatoid arthritis, osteoarthritis, acute pain, familial adenomatous polyposis and primary dysmenorrheal. Joshi *et al* compared a NLC-based gel of celecoxib with a micellar gel with the same composition, and found that the *in vitro* permeation of celecoxib from NLC gel was less than the permeation from the micellar based gel, confirming the sustained drug release from the NLC. *In vivo*, NLC gel produced significant higher edema inhibition, in comparison to the micellar gel (JOSHI and PATRAVALE, 2008; PARDEIKE, HOMMOSS, and MÜLLER, 2009).

Oral delivery systems occupy major portion of the drug delivery market. The use of colloidal carriers for oral administration enables to overcome important issues, such as low drug solubility, and poor absorption. A recent example of NLC for oral delivery is testosterone. The marketed product of testosterone (Andriol® Testocaps) is a soft gel capsule. Two capsules are required per single dose, due to the limited solubility of testosterone in oil. The act of swallowing two capsules may not be convenient to the patient, and could lead to a reduction in patient compliance. Hence, the goal was to incorporate testosterone in NLC, in order to obtain a similar or improved bioavailability, and to reduce the single dose to one capsule only. Hence, Muchow *et al* studied the bioavailability of testosterone loaded NLC in male Wistar rats in comparison with the commercial product in the non-fed state, and found that NLC showed a higher bioavailability (MUCHOW *et al.*, 2011; MÜLLER, SHEGOKAR, and KECK, 2011).

Despite the fact that parenteral administration of lipid nanoparticles represents a main challenge, there are already some pharmaceutical products commercialized such as AmBisome® (Amphotericin B), and Doxi®/Caelyx® (Doxorubicin) and DaunoXome® (Daunorubicin). Injectable lipid nanoparticles have been studied with anticancer drugs, imaging agents, anti-parkinsonism, antipsychotics and anti-rheumatoid arthritic agents, among others. In general, an improved bioavailability, enhanced anticancer efficacy and targeting have been observed. Liu *et al* developed docetaxel loaded-NLC to reduce toxicity and improve therapeutic efficacy for parenteral delivery. In comparison with Duopafei®, NLC revealed higher cytotoxicity against tumor cells (JOSHI and MÜLLER, 2009; Liu *et al.*, 2011; IQBAL *et al.*, 2012).

SLN and NLC have also been exploited for delivery of active compounds through the pulmonary, ocular and rectal route (UNER and YENER, 2007; MÜLLER, SHEGOKAR, and KECK, 2011; IQBAL *et al.*, 2012).

As mentioned before, the aim of this work was the optimization of properties for lipid nanoparticle, in particular SLN and NLC. Furthermore, to achieve optimum characteristics it is of great importance to establish the influence of multiple factors on the formulation properties, resorting to a limited number of experiments. The application of experimental design in this field has been increasing and has proven its usefulness (ZHANG, FAN, and SMITH, 2009; WOITISKI *et al.,* 2009). Chapter 4 details some experimental designs usually applied.

CHAPTER 4
EXPERIMENTAL DESIGN

Experimentation may be defined as the investigation of a defined area with a distinct objective, using appropriate tools and drawing conclusions that are justified by the experimental data so obtained (ARMSTRONG, 2006)[1].

Experimentation is carried out to determine the relationship between factors acting on the system and the response or properties of the system. The information is then used to pursue the aims of the project, with maximum efficiency. The resources available are optimized to reach the objectives as quickly and as surely as possible with the best possible precision (LEWIS, MATHIEU, and PHAN-TAN-LUU, 1999).

A blackbox approach may provide a better understanding on this issue (Figure 5). Considering a system (being a process, a product, or both) there are factors acting on the system, and thus affecting the respective response or output. The number of factors influencing the system is usually higher than the number of responses.

Figure 5. The blackbox view of a process or system, where the factors, F, control the response, *R*. Usually, n>>m.

Experimental design consists of planning having in view the optimization of the system. The process of optimizing a system relies on the description of the system on the basis of a response or responses determined by a set of factors. After defining the problem or experiment, the experimentalist should carefully define the factors to be evaluated, select a response, choose the experimental design, perform it, analyze the collected data and draw conclusions. The number of experiments necessary to identify the most relevant factors is one of the key issues to the experimentalist.

The determination of the experimental conditions may lead to the best value of the response measured. The investigation could lead to a target value, considered the optimal value for the response, or to an improvement of the results, without reaching a specific value.

[1] *This chapter relies frequently on ARMSTRONG, 2006.*

Usually, previous screening and factor studies enable better results for processes or formulations optimization. In particular, factor studies can indicate trends which show how a factor might be varied to favour a given response (LEWIS, MATHIEU, and PHAN-TAN-LUU, 1999).

Particularly, the development of pharmaceutical products is an expensive and complex process, involving many variables. Thus, it is reasonable to ask whether the process can be made more efficient, thereby reducing expenditure of time and money. More specifically, the development of a delivery system as nanoparticles involves important processes and variables that should be considered. Experimental design has been frequently applied for nanoparticle optimization, considering its advantages such as reduction in the number of experiments that need to be performed, development of mathematical models to assess the relevance and statistical significance of the factor effects, and evaluation of the interaction effect between the factors under study (FERREIRA *et al.*, 2007; WOITISKI *et al.*, 2009). Several approaches can be taken.

4.1. Factorial Design

A classical approach is to evaluate the effect of one experimental variable while keeping all other constant. However, the interaction between variables should not be ignored. When the effect of one factor depends on the level of another factor, the first will consequently be influenced by the magnitude of the other factor.

Factorial design allows the simultaneous evaluation of the factors and the assessment of their relative importance, and also the determination of interaction between them. By applying systematic changes in the factors, it is possible to assess the respective influence upon the response, as a means of separating those factors that are important from those that are not. This can be applied to many tasks in pharmaceutical issues, and forms the basis for many tests that seek to find an optimum solution. Systematic combinations of factors and levels are investigated, and all main effects and interactions evaluated. According to the objective of the experiment, the factors defined can be quantitative or qualitative, having numerical values or names, respectively. Each factor can be assigned a level which corresponds to a real value of the range of possible values for the factor. Both quantitative and qualitative factors may be set at 2 or more levels. The response is defined according to the experimental objectives.

The most common designs are the ones based on two levels for each factor. These are called full factorial design at two levels. In this case, 2^k experiments should be performed, being k the number of factors being assessed.

Considering a process with two variables, a full factorial design would require 2^2 experiments (Figure 6), resulting typically on a function with four parameters

$$R = \beta_0 + \beta_1 x_1 + \beta_2 x_2 + \beta_{12} x_1 x_2 \quad (1)$$

where R is the value of the response, x_1 and x_2 represent the two factors, and β_0 corresponds to the central point in a centered design, thus being given by the average value of the experiments in each level. The values of the two levels for each factor should be defined according to the range of work within the conditions of the experiment.

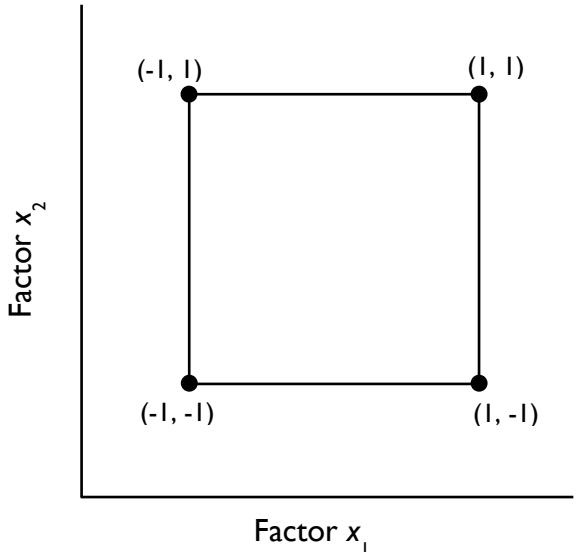

Figure 6. A full factorial design 2^2; two-level two-factor experimental design.

After carrying out the experiments, with two or three repetitions in all combinations of levels, a set of responses is obtained. Using a simple least squares procedure, the results obtained can be processed to predict optimal value for the response. According to the goal this could either be a minimum or a maximum. Currently, the calculation of the coefficients of the regression equation is carried out by computer with adequate statistical programs.

The application of coded levels for the independent variables allows an easier interpretation of the results. Usually, -1 is used for the lower level, and +1 is used for the higher one. The determination of the values of the coefficients defined above allows the evaluation of the importance of each factor chosen, as well as of the interaction.

When qualitative factors are used, the levels -1 and +1 could be coded as absence or presence of the respective factor, for instance. However, the estimation of optimum conditions involving all the variables is restricted to situations in which the qualitative factors are frozen.

As an example, consider a chemical reaction with two variables, temperature (x_1) and pressure (x_2) (adapted from PAIS, 2008). Table 3 presents the responses obtained from the applied design.

Table 3. Results from a chemical reaction in which two factors are studied (Adapted from PAIS, 2008).

Experiment	Temperature (°C)	Pressure (bar)	Yield (%)
1	40	5	90.5; 91.2
2	40	10	94.5; 93.9
3	80	5	89.5; 88.3
4	80	10	90.2; 90.8

Based on the two-level two-factor design described, the effect of temperature would correspond to the average of the effects this variable at the two levels of pressure (equation 2).

$$\beta_1 = \frac{1}{2}\{(\bar{R}_3 - \bar{R}_1) + (\bar{R}_4 - \bar{R}_2)\} \tag{2}$$

The interaction would be described as

$$\beta_{12} = \frac{1}{2}\{(\bar{R}_1 + \bar{R}_4) - (\bar{R}_2 + \bar{R}_3)\} \tag{3}$$

and is given by the difference between the value of the effect of temperature for the lower level of pressure and value of the effect of temperature for the higher level of pressure.

There is a systematic method for the calculation of the parameters described above. It starts by building a matrix that describes the experiments, *D*, and another one that describes the responses, *R*.

$$D = \begin{bmatrix} -1 & -1 \\ -1 & -1 \\ -1 & +1 \\ -1 & +1 \\ +1 & -1 \\ +1 & -1 \\ +1 & +1 \\ +1 & +1 \end{bmatrix} \qquad R = \begin{bmatrix} 90.5 \\ 91.2 \\ 94.5 \\ 93.9 \\ 89.5 \\ 88.3 \\ 90.2 \\ 90.8 \end{bmatrix}$$

The matrix *D* is then enlarged to the matrix *X*, following the order of parameters in the model function.

$$X = \begin{bmatrix} +1 & -1 & -1 & +1 \\ +1 & -1 & -1 & +1 \\ +1 & -1 & +1 & -1 \\ +1 & -1 & +1 & -1 \\ +1 & +1 & -1 & -1 \\ +1 & +1 & -1 & -1 \\ +1 & +1 & +1 & +1 \\ +1 & +1 & +1 & +1 \end{bmatrix}$$

The first column has unitary values, and corresponds to the independent term, the second has the values of the levels in factor 1, the third has the values of the levels in factor 2 and the fourth is the product of the values of factors 1 and 2.

When squares of the factors are comprised, there are columns with the square values of the levels. A simple succession of matrix operations would lead to the final model (4).

$$(X'X) = \begin{bmatrix} 8 & 0 & 0 & 0 \\ 0 & 8 & 0 & 0 \\ 0 & 0 & 8 & 0 \\ 0 & 0 & 0 & 8 \end{bmatrix} \qquad (X'R) = \begin{bmatrix} 728.9 \\ -11.3 \\ 9.9 \\ -3.5 \end{bmatrix}$$

$$a = (X'X)^{-1}(X'R) = \begin{bmatrix} 91.11 \\ -1.41 \\ 1.24 \\ -0.44 \end{bmatrix}$$

$$R = 91.11 - 1.41x_1 + 1.24x_2 - 0.44x_1x_2 \qquad (4)$$

This analysis is conducted easily with software available, such as the Octave (EATON, 2009).

In some cases, this model is not sufficient to perform a detailed description of the system. Thus, an improvement of the model used should be done in a more or less systematic way. The main effects should be considered in first place, then two-way interactions, squares of

main effects, three-way interaction, and so on. Though an increase in the number of parameters makes the model more unstable towards interpolation and extrapolation, it also increases the quality of fitting. Consequently, the number of experiments will increase.

4.2. PLACKETT-BURMAN DESIGN

When the number of factors to be evaluated increases, the application of a full factorial 2^k design requires an excessive number of experiments. To reduce the number of experiments, the Plackett-Burman design is often applied. Only the main effects are evaluated in this plan, allowing the determination of the few significant factors from a list of many potential ones. This was described in 1946 by R.L. Placket and J.P. Burman, and is based on statistics and combinatorial analysis. It may be used for *N* runs with *N*-1 factors (ARMSTRONG, 2006).

The design is obtained by writing the relevant line as a column. The next column is generated by moving the element down by one line and placing the last element in the first position (Table 4). Subsequent columns are prepared in the same way. The design is completed by adding a line of -1.

Table 4. A Plackett-Burman design for the study of eleven factors in twelve experiments (Adapted from ARMSTRONG, 2006).

Factor										
X_1	X_2	X_3	X_4	X_5	X_6	X_7	X_8	X_9	X_{10}	X_{11}
+1	-1	+1	-1	-1	-1	+1	+1	+1	-1	+1
+1	+1	-1	+1	-1	-1	-1	+1	+1	+1	-1
-1	+1	+1	-1	+1	-1	-1	-1	+1	+1	+1
+1	-1	+1	+1	-1	+1	-1	-1	-1	+1	+1
+1	+1	-1	+1	+1	-1	+1	-1	-1	-1	+1
+1	+1	+1	-1	+1	+1	-1	+1	-1	-1	-1
-1	+1	+1	+1	-1	+1	+1	-1	+1	-1	-1
-1	-1	+1	+1	+1	-1	+1	+1	-1	+1	-1
-1	-1	-1	+1	+1	+1	-1	+1	+1	-1	+1
+1	-1	-1	-1	+1	+1	+1	-1	+1	+1	-1
-1	+1	-1	-1	-1	+1	+1	+1	-1	+1	+1
-1	-1	-1	-1	-1	-1	-1	-1	-1	-1	-1

The Plackett-Burman design is very efficient if the main effects are considered dominant or interactions negligible. However, this type of design exhibits a high degree of confounding and cannot be used to evaluate individual main effects and interactions.

4.3. Central Composite Design

A central composite design is an extension of the full factorial 2^k design, and it is widely used in response-surface modeling and optimization. Starting with a 2^2 design, this can be extended by adding experiments to the design. Thus, a central experiment is placed in the center of the design and along the axes, at a distance α from the center point. This will provide information on how the response of interest is influenced by several variables, and a better control of the curvature of the response surface. Moreover, the description of the system will be improved due to the intermediate points (PAIS, 2008). By enlarging the number of possible coefficients, it allows to determine the optimal value for the response evaluated.

For a two-factor design, the experimental domain becomes a circle, centered on (0, 0) and passing through the factorial points (−1, −1) and (+1, −1). The position of the star points is given by $\alpha = 2^{N/4}$, where N is the number of factors. Thus, the axial points are situated at a distance of $\pm\sqrt{2}$ from the center point. Due to its shape, this is sometimes called "star design" (ARMSTRONG, 2006).

Central composite design can also be derived for more than two factors. For a three-factor two-level design, the experimental domain becomes a sphere, with six additional star points placed on the axes, and replicated points at the center of the design (Figure 7). Since the domain is a sphere another common choice is $\alpha = \sqrt{k}$, where k is the number of factors studied.

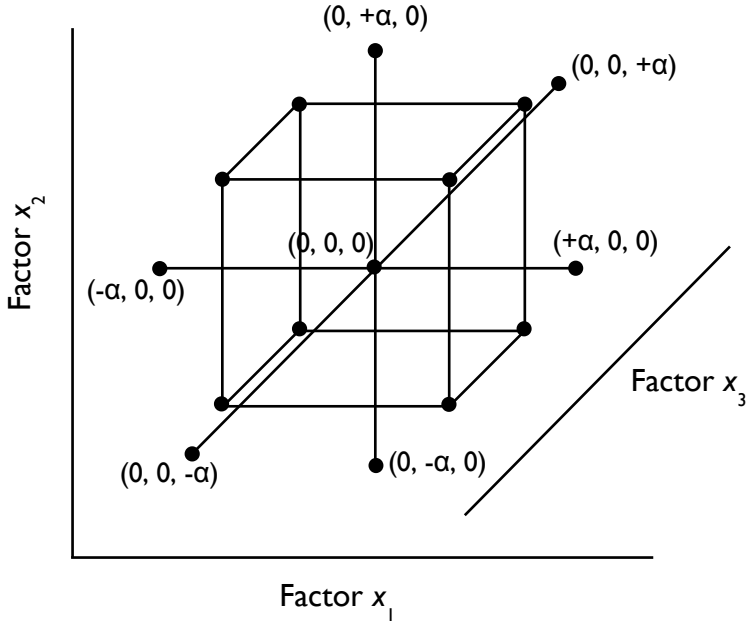

Figure 7. Central composite design for a three-factor experiment.

The application of this design requires a certainty that the values of the factors can be extended outside the range of conventional square or cubical design to encompass the star points. Thus, the position of the center point and the magnitude of each experimental unit must be chosen with care before experimentation begins, with the factorial points located well within the limits of each variable (ARMSTRONG, 2006).

Independently of the design executed, the significance of the coefficients obtained should be calculated. Student's *t*-test is commonly used, to assess the difference from null coefficients. However, this is only applicable to data with a normal distribution about the mean and true numerical values. Briefly, Student's *t*-test involves comparison of a value *t* calculated from the data with a tabulated value. If the calculated value exceeds the tabulated value, then a significant difference between the means of the two exists. The required level of significance, that is, the required value of *P*, should be defined in the beginning of the investigation. Usually, the value of *P* for physicochemical experiments is 0.05.

Considering two groups of data, *t* can be calculated by

$$t = \frac{x_{mA} - x_{mB}}{\sqrt{\left(\frac{s_A^2}{n_A} + \frac{s_B^2}{n_B}\right)}}$$

where x_{mA} and x_{mB} are the means of the group of data studied, n_A and n_B are the number of data points in each group, and S_A^2 and S_B^2 are the variances of the data from the group A and B, respectively.

CHAPTER 5
MATERIALS AND METHODS

5.1. LIPIDS

Precirol® ATO 5 (glyceryl palmitostearate) was kindly provided by Gattefossé (Saint-Priest, Cedex, France). It is a fine white powder with a melting point around 56°C. Precirol® ATO 5 is used in oral solid-dosage pharmaceutical formulations and as a lipophilic matrix for sustained release tablet and capsules formulations. It is also suitable for use in melting processing techniques such as spray cooling, hot melt coating and melt extrusion techniques for capsule and tablet filling. It is applied as well in coating techniques to provide taste masking and as a lubricating agent. The storage temperature must be below 18°C (ROWE, SHESKEY, and OWEN, 2006).

Miglyol® 812, a mixture of triglycerides of caprylic and capric acids, was acquired from Axo Industry (Wavre, Belgium). This lipid is used as an anti-sticking and polishing agent, and as a carrier, solvent and absorption promoter in oral products. For parenteral products it is used mainly as a carrier or solvent (COMPANY, 2013).

Oleic acid is a fatty acid that occurs naturally in various animal and vegetable fats and oils. It is used as an emulsifying agent in foods and topical pharmaceutical formulations. Oleic acid was acquired from Fluka (ROWE, SHESKEY, and OWEN, 2006).

Squalene is an all-trans isoprenoid containing six isoprene units, which is a naturally occurring substance found in human skin (HUANG *et al.*, 2008; FANG *et al.*, 2008). This was acquired from Sigma-Aldrich (Australia).

5.2. EMULSIFIERS

Tween® 80, or polisorbate 80, is a polyethylene sorbitol ester. Typically, the fatty acid composition is approximately 70% oleic acid with several other fatty acids such as palmitic acid. This emulsifier was acquired from Sigma-Aldrich (United Kingdom). Tween® 80 is a non-ionic surfactant widely used as emulsifying agent in the preparation of stable oil/water pharmaceutical emulsions, and can also be used as a solubilizing agent for a variety of substances including essential oils and oil-soluble vitamins, and as wetting agent in the formulation of oral and parenteral suspensions (ROWE, SHESKEY, and OWEN, 2006).

Lutrol® F 68 or Poloxamer 188 is a non-ionic surfactant obtained from BASF (Ludwigshafen, Germany). It is a polyoxyethylene-polyoxypropylene block copolymer used as emulsifying or solubilizing agent in oral, topical and parenteral preparations. Poloxamer 188 is suitable to prepare solid dispersions and to improve solubility, absorption and

bioavailability of low-solubility actives is solid oral dosage forms. It can also act as a co-emulsifier in creams and emulsions (ROWE, SHESKEY, and OWEN, 2006).

5.3. PORPHYRINS

Three different porphyrins were evaluated for incorporation on the optimized formulation: 5,10,15,20-tetraphenylporphyrin (TPP), 5,10,15,20-*tetrakis*(4-carboxyphenyl)porphyrin (B60) and 5,15-*bis*(3-hidroxiphenyl)porphyrin (MP-1046). These were synthetized as described elsewhere (JOHNSTONE *et al.*, 1996; NASCIMENTO, ROCHA GONÇALVES, and PINEIRO, 2010).

5.4. WATER

The water used in the experiments was purified (Millipore®) and filtered through a 0.22 µm nylon filter before use.

5.5. SOLVENTS

Toluene (SupraSolv®) was acquired from Merck (Darmstadt, Germany). This solvent was used in the experiments pertaining to the entrapment efficiency.

5.6. SOLUBILITY STUDIES

The solubility of the different porphyrins was determined in both solid and liquid lipids. For the solid lipid, 1g of Precirol® was melted 5–10°C above the melting point in a water bath with controlled temperature, and small amounts of porphyrin were added until precipitation occurs. For the liquid lipids, oleic acid, Miglyol® 812 and squalene, an excess of porphyrin was added to 1 mL of the respective lipid, and left under agitation for 48h, at 25°C. The samples were then centrifuged for 10 min at 13000 rpm in Minispin® (Eppendorf Ibérica S.L., Madrid, Spain), and the supernatant collected, and subsequently analyzed by fluorescence spectroscopy using a LS45 Fluorescence Spectrometer (PerkinElmer®, United Kingdom). Each sample was suitably diluted and analyzed in triplicate.

5.7. PORPHYRIN DETERMINATION

Porphyrin determination was performed by fluorimetry using a LS45 Fluorescence Spectrometer (PerkinElmer®, United Kingdom).

Fluorimetry consists of measuring the fluorescence of a certain compound. Fluorescence occurs when the compound molecules are excited by absorption of light at an appropriate

wavelength, followed by the emission of radiation of a different wavelength caused by the conversion of the molecules from the excited state to the ground state.

Briefly, a fluorometer generates the wavelength of light required to excite the molecule of interest; it selectively transmits the wavelength of light emitted, and then measures the intensity of the emitted light. The emitted light is proportional to the concentration of the drug being measured (up to a maximum concentration). Fluorescent compounds have two characteristic spectra: an excitation spectrum and an emission spectrum, which are often referred to as a compound's fluorescence signature or fingerprint, since no two compounds have the same spectra. Thus, fluorimetry is a highly specific and sensitive analytical technique.

Validation of the method for porphyrin determination was performed regarding the linearity, precision, accuracy, selectivity and sensitivity and stability. Calibration curves were obtained from a series of standard solutions of porphyrin in toluene, ranging from 0.011 to 0.066 µg/mL (SD within the marks). Figure 8 shows the obtained calibration curve, which was used for EE determination.

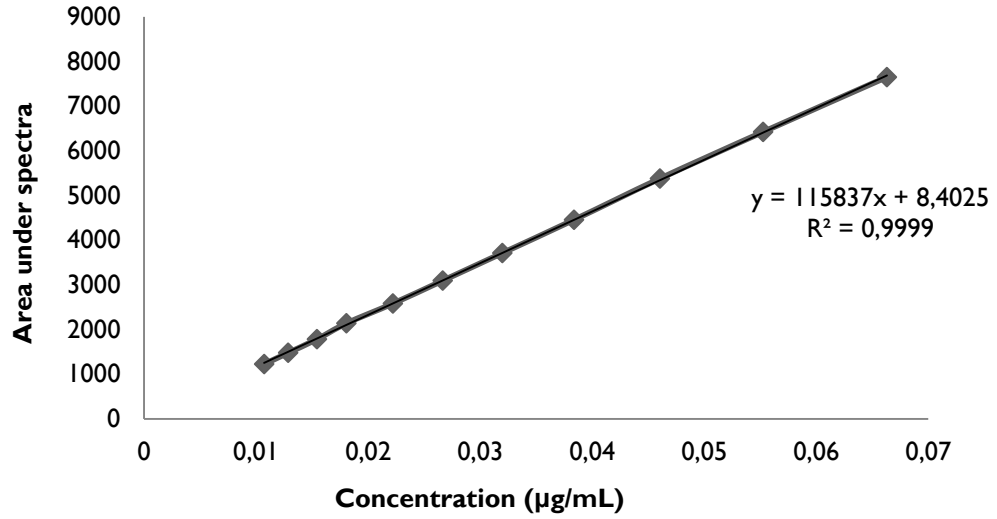

Figure 8. Calibration curve of porphyrin in toluene applied for EE determination.

The porphyrins studied were quantified in the liquid lipid, and in toluene, using the respective emission spectra.

5.8. PREPARATION OF SLN AND NLC

SLN and NLC were prepared by the hot high pressure homogenization (HPH) technique. A pre-emulsion was firstly obtained by the dispersion of the melted solid lipid and the liquid

lipid in 30 mL of a hot emulsifier solution at 70°C, using an Ultra-Turrax X1020 (Ystral GmbH D-7801, Dottingen, Germany) at 25000 rpm for 2 min. This hot pre-emulsion was thereafter submitted to high pressure homogenization using an Emulsiflex®-C3 (Avestin, Inc., Ottawa, Canada) at 1000 bar for 2 min 30 sec. The lipid dispersion obtained was subsequently refrigerated at 4°C to obtain the NLC.

When loaded nanoparticles were produced, a solution of porphyrin dissolved in the liquid lipid was prepared. The proper volume of this solution was added to the melted solid lipid. This method was applied to diminish the error on weighing the porphyrin, since the amount was very low.

5.9. Particle Size and Zeta Potential Measurements

Particle size was determined by photon correlation spectroscopy (PCS) which provides the mean particle size, and the respective polydispersity index (PI), a measure of the width of the distribution. PCS measures the fluctuation of the intensity of the scattered light which is caused by the motion of the particles, and is a suitable technique for application to particles ranging in size from a few nm to approximately 3 µm (MEHNERT and MÄDER, 2001). PCS was performed using a Delsa Nano C Submicron (Beckman Coulter, Krefeld, Germany) with a detection angle of 160°, at a temperature of 25°C. The samples were suitably diluted with ultrapurified water, and each value was measured in triplicate.

Laser diffractometry (LD) was also performed in order to detect the presence of microparticles. It resorted to a laser diffraction particle size analyzer (Beckman Coulter® LS 13.320, Miami, FL, USA), with polarization intensity differential scattering (PIDS). The instrument uses a Fraunhofer diffraction of laser scattered from particles in dispersion. LD measures the particle size distribution by measuring the angular variation in intensity of light scattered as a laser beam passes through a dispersed particulate sample. Smaller particles cause a more intense scattering at high angles, as compared to larger ones. This technique covers a broad size ranging from the nanometer to the lower millimeter range, and it is recommended to use it simultaneously with PCS (MEHNERT and MÄDER, 2001).

The real refractive index and the imaginary refractive index were set to 1.54 and 0.01, respectively. The LD data were expressed using volume distributions, and given as diameter values corresponding to percentiles of 10%, 50%, and 90%. The span value is a statistical parameter useful to characterize the particle size distribution, and was calculated using

$$\text{Span} = \frac{(d90\%-d10\%)}{d50\%}$$

A high value of span indicates a wide size distribution and, therefore, a high polydispersity (TEERANACHAIDEEKUL *et al.*, 2007).

The zeta potential value reflects the surface charge of the particle, and is a parameter very useful for the assessment of the physical stability of colloidal systems, as in general particle aggregation is less likely to occur for charged particles (high zeta potential) due to electric repulsion (MÜLLER, MÄDER, and GOHLA, 2000). To be considered stable, a zeta potential higher than | 30mV | is desirable (DOKTOROVOVA and SOUTO, 2009). Therefore, the value of this parameter was also determined by PCS using a Delsa Nano C Submicron (Beckman Coulter, Krefeld, Germany) at 25°C. Samples were adequately diluted with ultrapurified water.

5.10. Scanning Electronic Microscopy (SEM)

In order to investigate the morphology of the nanoparticles SEM analysis was performed. Prior to analysis, the sample was diluted with ultrapurified water, placed on a double-side carbon tape mounted onto an aluminium stud, and dried in a desiccator. The sample was then sputter coated with gold in order to make it conducting. SEM images were recorded on a Jeol, JSM-6010LV/6010LA (Tokyo, Japan) scanning electron microscope, with an acceleration voltage of 20kV.

5.11. Entrapment Efficiency and Drug Loading Determinations

The entrapment efficiency (EE) which corresponds to the amount of drug that can be incorporated in the nanoparticles, either inside the particle, or adsorbed at the respective surface was calculated indirectly by measuring the concentration of the free drug in the aqueous phase of the nanoparticle dispersion.

Firstly, for the determination of the total amount of porphyrin in the system, 1 mL of NLC loaded with porphyrin plus 9 mL of toluene were left under agitation for 30 min, at 80°C. The dispersion was then agitated in a vortex for 5 min, and centrifuged for 15 min at 3000 rpm in a Sigma® Laborzentrifugen 3K15. The supernatant was collected and subsequently analyzed by fluorescence spectroscopy using a LS45 Fluorescence Spectrometer (PerkinElmer®, United Kingdom). Each sample was suitably diluted and analyzed in triplicate.

The ultrafiltration-centrifugation method was applied, using centrifugal filters (Amicon® Ultra-4, Millipore, Germany) with a 100kDa molecular weight cut-off, to determine the amount of free drug in the aqueous dispersion. Briefly, 1mL of NLC loaded with porphyrin was placed into the upper chamber of the centrifuge filter, which was centrifuged at 4000×g for 90 min at 4°C. The amount of free drug in the aqueous dispersion phase collected in the outer chamber of the centrifugal filter after separation was determined by fluorescence spectroscopy (PerkinElmer®, United Kingdom). The EE was calculated following the equation

$$\%EE = \left(\frac{W_{initial\ drug} - W_{free\ drug}}{W_{initial\ drug}}\right) \times 100$$

where $W_{initial\ drug}$ is the amount of porphyrin added when the NLC were produced, and $W_{free\ drug}$ is the amount of drug determined in the aqueous phase after nanoparticles separation by ultrafiltration-centrifugation.

5.12. Experimental Design

In the present work, several experimental designs were performed in order to evaluate the influence of various composition variables in SLN and NLC formulations, and to optimize the systems. The factors investigated were the emulsifier concentration, the liquid lipid, and its absence or presence in the composition. As presented on Table 5, two different emulsifiers, one solid lipid and three different liquid lipids were assessed. Different concentrations of these components were also tested.

Table 5. Components investigated in order to optimize the NLC and SLN formulations.

Solid lipid	**Liquid lipid**	**Emulsifier**
Precirol® ATO 5	Oleic acid	Tween® 80
	Miglyol	Poloxamer 188
	Squalene	

The designs consisted of 32 runs of experiments, one for each set of conditions. The experimental designs performed are described below. GNU Octave software was used to run the experimental designs with programs developed by the authors (EATON, 2009).

5.12.1. DESIGN 1

In a first stage, a two-level, two-factor, full factorial 2^k design was performed to evaluate the influence of the liquid lipid and the different emulsifiers on nanoparticles. The responses defined were particle size and zeta potential.

The mathematic model used was

$$D = \beta_0 + \beta_1 x_1 + \beta_2 x_2 + \beta_{12} x_1 x_2 \quad (5)$$

The independent variables were the emulsifier concentration and the lipid concentration and were denoted in the equation as x_1 and, x_2 respectively. The combined term ($x_1 x_2$) describes the interaction between the selected variables. Each independent variable was coded with -1 and +1 levels. Level -1 corresponds to the lower value of each variable, and level +1 to the highest one (Table 6).

Table 6. Coded levels for the selected variables: emulsifier concentration %(w/v) and lipid concentration %(w/w).

Level	Emulsifier concentration %(w/v)	Lipid concentration %(w/w)
-1	1%	2.5%
+1	5%	7.5%

To evaluate the influence of each variable, the coefficients β_0, β_1, β_2 and β_{12} were determined. By evaluating the magnitude of each coefficient, it is possible to predict the effect of the respective variable on the system, in this case on particle size and zeta potential. The higher the magnitude of each coefficient, the higher is the respective main effect on the system. A coefficient with a positive sign indicates that an increase in the respective parameter leads to an increase in the response. For the analysis of the interaction coefficients, the response should be analyzed in terms of how the variation of one factor could modulate the effect of another factor.

5.12.2. DESIGN 2

The second experimental design was performed to evaluate the impact of the presence or absence of a liquid lipid in the formulation composition, along with the influence of the emulsifier and the lipid concentration. A two-level, three variable, full factorial 2^k design was executed for the optimization of the composition.

The mathematic model used was

$$D = \beta_0 + \beta_1 x_1 + \beta_2 x_2 + \beta_3 x_3 + \beta_{12} x_1 x_2 + \beta_{23} x_2 x_3 + \beta_{13} x_1 x_3 \quad (6)$$

The independent variables were the emulsifier concentration, the lipid concentration, and the absence or presence of a liquid lipid, and were denoted in the equation as x_1, x_2 and x_3, respectively. The combined terms describe the interaction between the selected variables. β_1, β_2 and β_3 are the coefficients of the respective independent variables, and β_{12}, β_{23} and β_{13} are the coefficients of the interaction terms. As dependent variable or response, *D*, particle size was selected. Each independent variable was coded with -1 and +1 levels. Level -1 corresponds to the lower value of each variable, and level +1 to the highest one (Table 7).

Table 7. Coded levels for the selected variables: emulsifier concentration %(w/v), lipid concentration %(w/w), and absence or presence of a liquid lipid.

Level	Emulsifier concentration %(w/v)	Lipid concentration %(w/w)	Absence or presence of liquid lipid
-1	1%	2.5%	Absence
+1	5%	7.5%	Presence

The components used for the SLN and NLC formulations were the same as those used in Design 1.

5.12.3. DESIGN 3

The results obtained from the previous designs (1 and 2) allowed a general prediction of the nanoparticle behavior according to the different components used. A third experimental design, a central composite design, was performed in order to obtain a fine tuning for the optimization of the system.

This consisted of a three-factor, two-level design, plus six star points on the axes and replicated points at the center of the design. The position of the "star" points is given by $\alpha = \sqrt{k}$, where *k* is the number of factors. To a better understanding of the position of the "star" points, Figure 9 presents a two dimensions image of the central composite design circumscribed applied here.

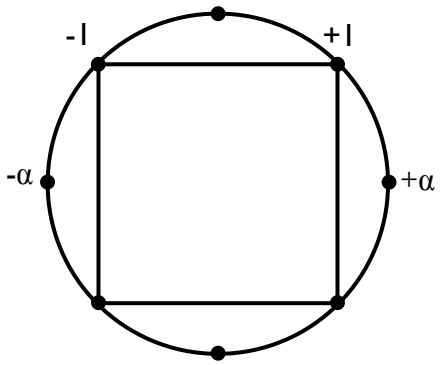

Figure 9. Central composite design circumscribed.

The emulsifier concentration (x_1), the liquid:solid lipid ratio (x_2), and lipid phase concentration (x_3) were the independent variables selected. Again, each independent variable was coded with -1 and +1 levels (Table 8).

Table 8. Coded values for the variables defined for the central composite design.

	x_1	x_2	x_3
Center point	0	0	0
Factorial points	-1	-1	-1
	-1	-1	+1
	-1	+1	-1
	+1	-1	-1
	+1	+1	-1
	+1	-1	+1
	-1	+1	+1
	+1	+1	+1
"star" points	- α	0	0
	+ α	0	0
	0	- α	0
	0	+ α	0
	0	0	- α
	0	0	+ α

The mathematic model used was

$$D = \beta_0 + \beta_1 x_1 + \beta_2 x_2 + \beta_3 x_3 + \beta_{12} x_1 x_2 + \beta_{23} x_2 x_3 + \beta_{13} x_1 x_3 + \beta_{11} x_1^2 + \beta_{22} x_2^2 + \beta_{33} x_3^2 + \beta_{123} x_1 x_2 x_3 \quad (7)$$

β_1, β_2 and β_3 are the coefficients of the independent variables, and β_{12}, β_{23} and β_{13} are the coefficients of the interaction terms. $\beta_{123} x_1 x_2 x_3$ describes the interaction between all the independent variables. These were estimated by least squares linear regression. As dependent variable or response, *D*, particle size was selected. The study of each coefficient and the respective interaction was performed, as in previous designs. The specific conditions investigated are presented on Table 9.

Table 9. Conditions investigated in the central composite design performed.

	- α	**-1**	**Center point**	**+1**	**+ α**
Tween® 80 Concentration %(w/v) x_1	1%	2%	3.5%	5%	6%
Liquid:Solid lipid ratio x_2	100:0	90:10	75:25	60:40	50:50
Lipid Phase Concentration %(w/w) x_3	2%	3%	4.5%	6%	7%

CHAPTER 6

OPTIMIZATION OF SLN AND NLC FORMULATIONS

6.1. Emulsifier and Lipid Selection for SLN and NLC Preparation

The choice of emulsifier and the respective concentration is a very important step in SLN and NLC production due to its influence in particle size and dispersion stability (VITORINO *et al.*, 2011). The behavior of the nanoparticles may differ considerably due to the very small size of the particles and the high amount of surfactant which is necessary to stabilize the colloidal lipid dispersion. High concentrations of emulsifier reduce the surface tension and facilitate the particle partition during homogenization. An increase in surface area is associated with a decrease in particle size (MEHNERT and MÄDER, 2001). In the present work, two emulsifying agents were evaluated for the production of SLN and NLC, composed by different lipids.

According to the lipid used, different parameters can influence nanoparticle formation. The velocity of lipid crystallization, lipid hydrophilicity and the shape of the crystal lipids are some examples. The lipid composition might also have considerable impact on the quality of the dispersion obtained. Lipids which form highly crystalline particles with a perfect lattice lead to drug expulsion. More complex lipids being mixtures of mono-, di- and triglycerides and also containing fatty acids of different chain length form less perfect crystals with many imperfections offering space to accommodate the drug (MÜLLER, MÄDER, and GOHLA, 2000). Increasing the lipid content over 5-10% results, in most cases, in larger particles and broader size distributions (MEHNERT and MÄDER, 2001).

NLC and SLN were produced by high pressure homogenization (hot technique) and the composition studied is presented on Table 10. For the NLC produced the liquid:solid lipid ratio used was 50:50. Precirol® ATO 5 was selected as the solid lipid, and oleic acid, Miglyol® 812 and squalene for the liquid lipids. Tween® 80 and Lutrol® F 68, or Poloxamer 188, were selected as emulsifiers. The combination of Precirol® and oleic acid, Miglyol® 812 and squalene will be referred as NLC-PO, NLC-PM and NLC-PS, respectively.

Table 10. Composition of NLC and SLN under study.

Lipid Concentration %(w/w)	Tween® 80 %(w/v)	Poloxamer 188 %(w/v)
2.5%	1%	-
	5%	-
	-	1%
	-	5%
7.5%	1%	-
	5%	-
	-	1%
	-	5%

6.2. Particle Size and Zeta Potential Measurements

The particle size and polydispersity index were determined by PCS, as mentioned before, and the results obtained are presented in Table 11. The analysis of these is important to a better understanding of the influence of the composition in the particle size.

In a first analysis of the data, there are some interesting results. All the formulations tested have different size distributions. It is clear that the liquid:solid lipid ratio is an important parameter for particle size, as it can be seen that an exclusively solid lipid matrix (SLN) lead to larger diameter particles.

The differences determined by the emulsifiers used are also noticeable. In general, a higher emulsifier concentration leads to smaller particle size. The combination of oleic acid and the emulsifier Poloxamer 188 lead to larger particle size, whereas the use of Tween® 80 produced smaller particles. The polydispersity indexes obtained were quite similar in the NLC formulation. However, SLN presented the highest values of PI, usually higher than 0.3, revealing a broader size distribution, while the NLC formulations presented PI values lower than 0.3. According to the literature, nanoparticles characterized by a PI value lower than 0.3 can be accepted (ZHANG, FAN, and SMITH, 2009; IQBAL *et al.*, 2012).

Table 11. Mean particle size of different compositions studied for NLC and SLN. T1: Tween® 80 1%(w/v); T5: Tween® 80 5%(w/v); P1: Poloxamer 188 1%(w/v); P5: Poloxamer 188 5%(w/v). Values represented as mean ± SD (*n*=3).

Formulation	Lipid Concentration %(w/w)	Emulsifier	Particle Size (nm)	PI
NLC-PO	2.5%	T1	293 ± 33	0.198 ± 0.04
		T5	132 ± 2	0.309 ± 0.008
		P1	321 ± 25	0.21 ± 0.06
		P5	444 ± 5	0.236 ± 0.005
	7.5%	T1	430 ± 16	0.224 ± 0.008
		T5	146.2 ± 0.9	0.273 ± 0.002
		P1	389 ± 23	0.181 ± 0.007
		P5	651 ± 91	0.28 ± 0.04
NLC-PM	2.5%	T1	183 ± 2	0.294 ± 0.011
		T5	277 ± 4	0.272 ± 0.009
		P1	254 ± 11	0.26 ± 0.04
		P5	262 ± 6	0.273 ± 0.003
	7.5%	T1	247 ± 6	0.30 ± 0.02
		T5	269 ± 4	0.295 ± 0.011
		P1	349 ± 42	0.24 ± 0.06
		P5	235 ± 3	0.290 ± 0.005
NLC-PS	2.5%	T1	308 ± 4	0.301 ± 0.014
		T5	238 ± 5	0.29 ± 0.03
		P1	388 ± 22	0.180 ± 0.008
		P5	324 ± 7	0.26 ± 0.03
	7.5%	T1	253 ± 2	0.292 ± 0.007
		T5	226 ± 1	0.287 ± 0.012
		P1	398 ± 90	0.18 ± 0.04
		P5	286 ± 11	0.26 ± 0.04
SLN	2.5%	T1	420 ± 33	0.30 ± 0.04
		T5	315 ± 60	0.21 ± 0.04
		P1	788 ± 409	0.33 ± 0.13
		P5	927 ± 354	0.34 ± 0.08
	7.5%	T1	521 ± 94	0.30 ± 0.02
		T5	327 ± 82	0.275 ± 0.017
		P1	1601 ± 617	0.5 ± 0.2
		P5	864 ± 219	0.34 ± 0.06

Of all the liquid lipids used, the formulation with oleic acid (NLC-PO) displayed the smaller particle sizes (132 ± 2), but also the largest ones (651 ± 91). In this preliminary analysis, this formulation was the one where the emulsifier and its concentration revealed a more prominent effect on the particle size obtained. Both NLC-PM and NLC-PS formulations have a more homogenous particle size distribution, where the emulsifier and the respective concentration do not appear to have a marked effect on the particle size obtained.

Zeta potential was also determined by PCS and the values obtained are presented in Table 12. Zeta potential corresponds to the surface charge of the particles. The respective measurement allows for predictions of stability of colloidal dispersions. In general, the formulations produced are stable, with only a few values below | 30mV |.

The highest zeta potential value was obtained for the NLC-PO formulation with the lower lipid content and Tween® 80 concentration. This was also the conditions determining more pronounced fluctuations. For the lower lipid concentration (2.5%), the increase in Tween® 80 concentration altered considerably the zeta potential of the formulation from -42 ± 2 to -18 ± 1. However, for the higher lipid concentration (7.5%) the same alteration did not lead to a significant change in the zeta potential value. This is also observed in the NLC-PM formulation. For the NLC-PS formulation, the lipid:emulsifier ratio did not result on a significant alteration of the zeta potential values.

Generally, the use of Poloxamer 188 resulted in higher zeta potential values, in comparison with Tween® 80. A lower emulsifier concentration usually resulted in higher zeta potential values.

The lipid concentration did not promote a notable change in the zeta potential values. In general, for the lower lipid concentration Poloxamer 188 produced more stable particles.

Both particle size and zeta potential preliminary results provided important information about the systems studied. However, these data are not sufficient to fine-tune an optimal formulation. Hence, these were used to perform different factorial designs in order to optimize the nanoparticle formulation. To evaluate the influence of the different factors in the system, the formulation, several experimental designs were applied.

Table 12. Zeta potential values (mean ± SD (*n*=3)) obtained for the different compositions studied for NLC and SLN. Key as in Table 11.

Formulation	Lipid Concentration %(w/w)	Emulsifier	Zeta Potential (mV)
NLC-PO	2.5%	T1	-42 ± 2
		T5	-18 ± 1
		P1	-28.2 ± 0.5
		P5	-30.2 ± 0.3
	7.5%	T1	-26.9 ± 0.3
		T5	-34.20 ± 0.8
		P1	-29.4 ± 0.3
		P5	-29.5 ± 0.4
NLC-PM	2.5%	T1	-24 ± 5
		T5	-18.3 ± 0.5
		P1	-32 ± 1
		P5	-29.5 ± 0.3
	7.5%	T1	-24.8 ± 0.7
		T5	-20.5 ± 0.3
		P1	-33 ± 1
		P5	-30.2 ± 0.8
NLC-PS	2.5%	T1	-22.8 ± 0.5
		T5	-20.9 ± 1.1
		P1	-33.4 ± 1.4
		P5	-26.2 ± 1.0
	7.5%	T1	-22.4 ± 0.2
		T5	-21.9 ± 0.3
		P1	-31.0 ± 0.9
		P5	-30.4 ± 0.4
SLN	2.5%	T1	-23 ± 4
		T5	-17 ± 3
		P1	-33 ± 2
		P5	-34.7 ± 1.5
	7.5%	T1	-24 ± 3
		T5	-19 ± 3
		P1	-31.2 ± 0.5
		P5	-32.2 ± 1.1

6.3. DESIGN 1

As stated on Chapter 5, the first experimental design performed was a two-level, two-factor, full factorial 2^k design with the purpose of evaluating the influence of the emulsifier concentration (x_1), using Tween® 80 and Poloxamer 188, and the lipid concentration (x_2) on the system. As dependent variables or responses, *D*, particle size and zeta potential were selected. To verify the statistical significance of the coefficients, *t*-tests were performed using a 95% (α=0.05) level of significance. Tables 13 and 14 gather the values of the coefficients obtained for the 2^2 design, related to the particle size, for Tween® 80 and Poloxamer 188, respectively, as well as the level of confidence. The Student's *t*-test analysis showed that the parameters are highly significant, with the exception of the β_2 and β_{12} coefficients for SLN produced with Tween® 80 and the NLC-PS formulation produced with Poloxamer 188.

In a first analysis of these results, particle size showed to be strongly influenced by the variables selected. In general, the emulsifier concentration (x_1) was the parameter with higher magnitude, but depending on the emulsifiers used different results are observed. Thus, their effect on the system should be analyzed carefully.

In general, the coefficients obtained vary with the emulsifier, being lower for Tween® 80. Analyzing the β_0 values of both emulsifiers, the values obtained for Tween® 80 are lower than for Poloxamer 188, showing that the use of Tween® 80 will produce, on average, smaller particles, as observed on the preliminary assessment of the particle size measurements. Notice that, for SLN produced with Poloxamer 188, this coefficient was the only one with statistical significance, and highest magnitude.

The lipid concentration (x_2) was also an important variable. For both emulsifiers, a higher lipid concentration contributes to larger particle size, except for the NLC-PS formulation where this coefficient has a negative sign. This parameter had a higher magnitude for the SLN produced with both emulsifiers, confirming that an entirely solid lipid matrix (SLN) leads to larger diameter particles. However, it should be noticed that β_2 was not considered statistical significant for SLN produced with both emulsifiers.

The liquid:solid lipid ratio also represents a key parameter for particle size, as seen by the difference on β_0 values between the SLN and NLC formulations.

Table 13. Coefficients for particle size obtained from the 2^2 design applied for the formulations produced with Tween® 80.

Tween® 80	β_0	β_1	β_2	β_{12}
NLC-PO	250.40	-111.40	37.92	-30.68
***t*-value**	46.49	-20.68	7.04	-5.70
Level of confidence	100.00	100.00	99.99	99.95
NLC-PM	243.84	28.89	13.99	-18.09
***t*-value**	211.33	25.04	12.13	-15.68
Level of confidence	100.00	100.00	100.00	100.00
NLC-PS	256.08	-24.33	-16.62	10.90
***t*-value**	280.46	-26.65	-18.20	11.94
Level of confidence	100.00	100.00	100.00	100.00
SLN	394.42	-73.52	27.16	-20.75
***t*-value**	18.31	-3.41	1.26	-0.96
Level of confidence	100.00	99.08	75.72	63.64

Table 14. Coefficients for particle size obtained from the 2^2 design applied for the formulations produced with Poloxamer 188.

Poloxamer 188	β_0	β_1	β_2	β_{12}
NLC-PO	451.26	96.16	68.54	34.64
***t*-value**	32.22	6.87	4.89	2.47
Level of confidence	100.00	99.99	99.88	96.15
NLC-PM	274.69	-26.41	17.08	-30.33
***t*-value**	43.13	-4.15	2.68	-4.76
Level of confidence	100.00	99.68	97.21	99.86
NLC-PS	348.83	-43.78	-6.98	-11.87
***t*-value**	25.77	-3.23	-0.52	-0.88
Level of confidence	100.00	98.80	38.02	59.38
SLN	1045.09	-149.29	187.64	-219.02
***t*-value**	8.52	-1.22	1.53	-1.79
Level of confidence	100.00	74.18	83.54	88.80

The interaction between the variables defined cannot be neglected. It is important to assess how the effect of one factor will be influenced by changes in the levels of another. The following analysis can be applied as many times as it is necessary.

Considering the results for Tween® 80 and the two variables previously defined, x_1 and x_2, we have the effect of x_1 given by

$$(\beta_1 + \beta_{12} x_2) x_1$$

For the formulation produced with oleic acid, NLC-PO, and SLN, the coefficients β_1 and β_{12} have negative signs. This approach allows concluding that for a higher emulsifier concentration ($x_1 = +1$) the interaction will reinforce its negative contribution, thus leading to a smaller particle size. Despite the observation of this trend, β_2 and β_{12} coefficients for SLN were not considered statistical significant.

The influence of the lipid concentration (x_2) can also be analyzed applying the same method. Considering the NLC-PO and NLC-PM produced with the same emulsifier we have

$$(\beta_2 + \beta_{12} x_1) x_2$$

Since the coefficient β_2 has a positive sign and β_{12} a negative one, for a higher lipid concentration ($x_2 = +1$) the interaction will decrease the positive influence of this factor, consequently leading to a slight reduction of particle size.

Different results are observed if NLC-PS is considered, for the same emulsifier. Here, the coefficient β_2 has a negative sign and β_{12} has a positive one. Hence, in a formulation with a higher emulsifier concentration ($x_1 = +1$), the (negative) effect of an increase in the lipid concentration ($x_2 = +1$) will be reversed by the interaction.

Regarding the formulations produced with Poloxamer 188, the same inspection can be done. In example, for the NLC-PO all the coefficients have positive signs. In this case, for a higher emulsifier concentration ($x_1 = +1$) the interaction will reinforce its positive contribution, thus leading to larger particles.

In comparison to NLC, SLN lead to larger particles as mentioned before and confirmed by the results from the analysis above. Although the only coefficient statistical significant for SLN produced with Poloxamer 188 is β_0, this has the highest magnitude for all remain conditions as well. Thus, in general, the use of Poloxamer 188 will produced larger particles in comparison with Tween® 80.

These results demonstrate that particle size is strongly influenced by the emulsifier and lipid concentration. Since the desirable formulation should have smaller particle size, the SLN were not considered for further study.

The coefficient values obtained for the 2^2 design, related to the second response studied, for both emulsifiers, as well as the level of confidence, are presented in Table 15 and 16.

For all the conditions evaluated with Tween® 80, β_1 has a positive sign and β_2 a negative one. Thus, an increase in emulsifier concentration (x_1) will lead to a less negative zeta potential value, and a decrease in lipid concentration (x_2) will lead to a more negative value. The interaction coefficient is more pronounced for the NLC-PO formulation. Here, the interaction will decrease the effect of a higher emulsifier concentration, leading to less stable particles. Yet, it should be noticed that the coefficients obtained for the second variable were not statistical significant, as well as the interaction coefficient β_{12}, with exception for NLC-PO formulation.

Table 15. Coefficients for zeta potential obtained from the 2^2 design applied for the formulations produced with Tween® 80.

Tween® 80	β_0	β_1	β_2	β_{12}
NLC-PO	-30.18	4.18	-0.40	-7.80
***t*-value**	-82.16	11.39	-1.09	-21.23
Level of confidence	100.00	100.00	69.12	100.00
NLC-PM	-21.81	2.42	-0.83	-0.27
***t*-value**	-27.60	3.06	-1.05	-0.35
Level of confidence	100.00	98.45	67.40	26.17
NLC-PS	-22.01	0.57	-0.11	-0.34
***t*-value**	-122.21	3.16	-0.61	-1.88
Level of confidence	100.00	98.66	43.88	90.36
SLN	-20.57	2.67	-0.54	-0.32
***t*-value**	-22.77	2.96	-0.59	-0.36
Level of confidence	100.00	98.17	43.16	26.86

Table 16. Coefficients for zeta potential obtained from the 2^2 design applied for the formulations produced with Poloxamer 188.

Poloxamer 188	β_0	β_1	β_2	β_{12}
NLC-PO	-29.33	-0.53	-0.10	0.51
***t*-value**	-266.95	-4.85	-0.89	4.65
Level of confidence	100.00	99.87	59.92	99.84
NLC-PM	-31.01	1.17	-0.27	-0.07
***t*-value**	-120.01	4.52	-1.05	-0.25
Level of confidence	100.00	99.81	67.76	19.47
NLC-PS	-30.28	1.96	-0.45	-1.64
***t*-value**	-104.17	6.74	-1.54	-5.65
Level of confidence	100.00	99.99	83.85	99.95
SLN	-32.81	-0.65	1.13	0.16
***t*-value**	-83.71	-1.65	2.88	0.42
Level of confidence	100.00	86.22	97.94	31.32

As for the conditions assessed with Poloxamer 188, the conclusions are distinct. For NLC-PO formulation and SLN, a higher emulsifier concentration (x_1) will lead to a more negative zeta potential value, and thus more stable particles. The interaction coefficients have very small magnitude. For NLC-PM and NLC-PS, a higher emulsifier concentration (x_1) will lead to a less negative zeta potential value. An increase in lipid concentration (x_2) will lead to more stable particles. Nevertheless, it should not be forgotten that the coefficient for this variable was only statistical significant for the SLN produced with Poloxamer.

In general, to achieve smaller particles the emulsifier concentration should be increase and the lipid concentration reduced. However, these conditions would result on particles with reduced stability. Thus, zeta potential values are not in agreement with particle size results. Therefore, further study was necessary to achieve optimal results.

6.4. DESIGN 2

Along with other variables, to assess the influence of the presence or absence of a liquid lipid, in particular, a second experimental design was accomplished. A two-level, three variable, full factorial 2^k design was applied. Again, both emulsifiers were used. The emulsifier concentration (x_1), the lipid concentration (x_2), and the absence or presence of a liquid lipid (x_3) were the independent variables selected. As dependent variable or response, *D*, particle

size and zeta potential were defined. Table 17 and 18 presents the values of the coefficients obtained for the 2^3 design, as well as the level of confidence.

Table 17. Coefficients for particle size obtained from the 2^3 planning applied in order to evaluate the influence of the mentioned variables for Tween® 80.

Tween® 80	β_0	β_1	β_2	β_3	β_{12}	β_{23}	β_{13}
NLC-PO	323.08	-93.13	33.21	-72.68	-26.39	4.70	-18.27
***t*-value**	31.09	-8.96	3.20	-6.99	-2.54	0.45	-1.76
Level of confidence	100.00	100.00	99.47	100.00	97.88	34.34	90.32
NLC-PM	319.80	-22.99	21.25	-75.96	-20.10	-7.26	51.88
***t*-value**	31.88	-2.29	2.12	-7.57	-2.00	-0.72	5.17
Level of confidence	100.00	96.50	95.08	100.00	93.86	52.08	99.99
NLC-PS	325.93	-49.60	5.95	-69.84	-5.60	-22.56	25.27
***t*-value**	30.22	-4.60	0.55	-6.48	-0.52	-2.09	2.34
Level of confidence	100.00	99.97	41.15	100.00	38.97	94.83	96.84

Table 18. Coefficients for particle size obtained from the 2^3 planning applied in order to evaluate the influence of the mentioned variables for Poloxamer 188.

Poloxamer 188	β_0	β_1	β_2	β_3	β_{12}	β_{23}	β_{13}
NLC-PO	748.17	-26.57	128.09	-296.91	-92.19	-59.55	122.73
***t*-value**	11.11	-0.39	1.90	-4.41	-1.37	-0.88	1.82
Level of confidence	100.00	30.20	92.59	99.96	81.13	61.13	91.41
NLC-PM	659.89	-87.85	102.36	-385.20	-124.67	-85.28	61.44
***t*-value**	10.34	-1.38	1.60	-6.04	-1.95	-1.34	0.96
Level of confidence	100.00	81.35	87.29	100.00	93.26	80.10	65.09
NLC-PS	696.96	-96.54	90.33	-348.13	-115.44	-97.31	52.75
***t*-value**	10.74	-1.49	1.39	-5.36	-1.78	-1.50	0.81
Level of confidence	100.00	84.47	81.80	100.00	90.68	84.78	57.24

For Tween® 80, the main parameters influencing the system were the emulsifier concentration (x_1) and the presence of a liquid lipid (x_3), as it can be seen by the higher magnitude of the respective coefficients. As for Poloxamer 188, the lipid concentration (x_2) and the presence of a liquid lipid (x_3) were the main parameters influencing the system. β_1 has a negative sign for all conditions tested, showing that a higher emulsifier concentration

will produce smaller particles, as seen as well in the first design performed. As for β_2, it has a positive sign in all the conditions analyzed, revealing the positive effect of this variable in particle size. An increase in lipid concentration leads to larger particle diameter. β_3 has a negative sign for all conditions tested, from which we can conclude that the presence of liquid lipid is crucial for reduction of particle size. However, the magnitude of the coefficients differ with the different emulsifiers.

Generally, in comparison to Tween® 80, Poloxamer 188 displayed higher coefficient values, particularly for β_0, thus confirming the preliminary results of particle size measurements suggesting that Poloxamer 188 produces larger particles. For this emulsifier, the lipid concentration (x_2) is a parameter of great importance. A higher lipid concentration leads to larger particle size. The high magnitude of the third variable (β_3) indicates the pronounced effect of the presence of a liquid lipid on particle size for the formulations produced with Poloxamer 188.

The other emulsifier investigated, Tween® 80, lead to smaller particles, as previously mentioned. Thus, the respective results should be analyzed more carefully.

For Tween® 80, the NLC-PO formulation possesses the highest values for the parameters β_1 and β_2. Relative to the other liquid lipids, the third variable (β_3) is similar. The emulsifier concentration (x_1) determines a negative effect on particle size, as well as the presence of oleic acid. A higher emulsifier concentration will thus produce smaller particles, as well as the presence of the liquid lipid (x_3). Among all the liquid lipids used, oleic acid is the one with the higher magnitude for the β_2 coefficient showing that an increase in the lipid concentration will produce an increase in particle size. Moreover, the isolated parameters produced a more pronounced effect than the respective interactions.

For analyzing the interaction effects, the approach used previously is applied again. As mentioned before, the lipid concentration is a key parameter, and a higher value for this parameter increases particle size. Focusing now on the interaction between the emulsifier concentration (x_1) and the lipid concentration (x_2), the parameter β_2 is positive and β_{12} is negative, for all the conditions investigated. Thus, a higher emulsifier concentration ($x_1 = +1$), will decrease the positive influence of the lipid concentration (x_2), since $\beta_{12}x_1x_2<0$, leading to a smaller size particle. Yet, the only condition were this coefficient was statistical significant was for NLC-PO.

Considering now the interaction between the emulsifier concentration (x_1) and the presence or absence of a liquid lipid (x_3), both coefficients have negative signs for NLC-PO, regarding Tween® 80. Considering the absence of liquid lipid ($x_3 = -1$) and a higher emulsifier concentration ($x_1 = +1$), the interaction will decrease the negative effect of the latter variable. On the other hand, the introduction of a liquid lipid ($x_3 = +1$) will reinforce the effect of a higher emulsifier concentration, decreasing particle size.

For this specific condition, β_{23} have a small magnitude, and therefore we can conclude that the interaction between the presence of liquid lipid (x_3) and the lipid concentration (x_2) is negligible. Moreover, this was the only coefficient with no statistical significance for all the conditions assessed.

Regarding the same emulsifier, for the other formulations, β_{13} has a positive sign. Hence, considering only the parameters x_1 and x_3, a higher emulsifier concentration will decrease particle size, as seen from Design I. However, for these conditions, the introduction of a liquid lipid ($x_3 = +1$) in a formulation with a higher emulsifier concentration ($x_1 = +1$) will reduce the effect of the latter parameter in particle size. Hence, to decrease particle size, the liquid lipid should be introduced in a formulation with a lower emulsifier concentration.

Regarding the formulations composed with squalene and Miglyol® 812, using Tween® 80 as emulsifier, these exhibited the lowest values for β_2, showing that the lipid concentration (x_2) has not a strong effect on particle size, when this liquid lipids are applied. In fact, for these conditions, the presence of the liquid lipid (x_3) was the coefficient with the highest magnitude. Thus, the presence of these liquid lipids, as well as a higher emulsifier concentration, tends to decrease particle size.

In NLC-PS, β_{12} is small and do not have statistical significance. Therefore, we can conclude that the interaction between the emulsifier concentration (x_1) and the lipid concentration (x_2) is reduced.

Focusing on the interaction between the lipid concentration (x_2) and the presence or absence of a liquid lipid (x_3), for NLC-PM and NLC-PS, both β_3 and β_{13} coefficients have negative signs. In the presence of the liquid lipid ($x_3 = +1$), and a higher lipid concentration ($x_2 = +1$), the interaction will reinforce the negative effect of the presence of the liquid lipid, decreasing particle size.

The same 2^3 design was applied to zeta potential. Table 19 and 20 presents the values of the coefficients obtained for the 2^3 design, as well as the level of confidence.

Table 19. Coefficients for zeta potential obtained from the 2^3 design applied for the formulations produced with Tween® 80.

Tween® 80	β_0	β_1	β_2	β_3	β_{12}	β_{23}	β_{13}
NLC-PO	-25.37	3.43	-0.47	-4.81	-4.06	0.07	0.76
***t*-value**	-24.81	3.35	-0.46	-4.70	-3.97	0.07	0.74
Level of confidence	100.00	99.62	34.71	99.98	99.90	5.30	53.04
NLC-PM	-21.19	2.54	-0.68	-0.62	-0.30	-0.14	-0.12
***t*-value**	-36.40	4.37	-1.17	-1.07	-0.51	-0.25	-0.21
Level of confidence	100.00	99.96	74.25	69.95	38.38	19.34	16.71
NLC-PS	-21.29	1.62	-0.32	-0.72	-0.33	0.21	-1.05
***t*-value**	-47.66	3.62	-0.72	-1.62	-0.74	0.48	-2.35
Level of confidence	100.00	99.79	52.08	87.56	53.00	36.20	96.89

Table 20. Coefficients for zeta potential obtained from the 2^3 design applied for the formulations produced with Poloxamer 188.

Poloxamer 188	β_0	β_1	β_2	β_3	β_{12}	β_{23}	β_{13}
NLC-PO	-31.07	-0.59	0.52	1.74	0.34	-0.61	0.06
***t*-value**	-153.92	-2.92	2.55	8.61	1.67	-3.04	0.28
Level of confidence	100.00	99.04	97.94	100.00	88.70	99.25	21.82
NLC-PM	-31.91	0.26	0.43	0.90	0.05	-0.70	0.91
***t*-value**	-139.10	1.14	1.86	3.92	0.21	-3.05	3.95
Level of confidence	100.00	72.85	92.04	99.89	16.67	99.28	99.90
NLC-PS	-31.54	0.66	0.34	1.27	-0.74	-0.79	1.30
***t*-value**	-97.78	2.04	1.05	3.92	-2.29	-2.44	4.04
Level of confidence	100.00	94.24	69.30	99.89	96.52	97.42	99.92

For Tween® 80 the main parameters influencing zeta potential were the emulsifier concentration (x_1) and the absence or presence of a liquid lipid (x_3). For Poloxamer 188, the third variable had the pronounced influence on the response. Nevertheless, the coefficients have very small magnitude.

For the first emulsifier studied, β_1 has a positive sign, and β_2 and β_3 have negative signs. Thus, an increase in emulsifier concentration (x_1) will lead to a less negative zeta potential value, and a decrease in lipid concentration (x_2) will lead to a more negative value. The

presence of a liquid lipid contributes to more negative values of zeta potential. Of all the interactions evaluated, the more pronounced is the interaction between the emulsifier concentration (x_1) and the lipid concentration (x_2), for the NLC-PO formulation. In this case, the interaction will reinforce the positive effect of the emulsifier concentration, and will decrease the negative effect of the second variable.

For the formulations produced with Poloxamer 188, the presence of a liquid lipid was the main variable influencing the system, leading to less negative values of zeta potential. This was also the only parameter with statistical significance for all the formulations produced with this emulsifier. An increase in the lipid concentration will also lead to less negative values of zeta potential. NLC-PO was the only condition with a negative β_1 coefficient. Hence, for the mentioned condition, an increase in Poloxamer 188 concentration will lead to more stable particles.

Despite the fact that the β_0 had a higher magnitude for the formulations produced with Poloxamer 188, which indicate that this emulsifier would produce a stable dispersion, the variables have, in general, a negative and stronger effect on zeta potential of the formulations produced with Tween® 80. This enables some control of the variables studied in order to achieve a good stability of the dispersion.

Regarding both responses studied, there are some interesting outcomes from this investigation. Particle size is strongly influenced by the variables selected. In general, Poloxamer 188 will lead to an increase in particle size, conversely to Tween® 80. Particularly, in the formulations composed by oleic acid and Tween® 80 the variables studied have a pronounced effect, and allowed the production of smaller particles, as previously observed. Also, Tween® 80 provided fair stability to the dispersion produced. It was observed from both designs that the variables defined do not have a noticeable influence on zeta potential of the dispersion produced. Thus, for the optimization process, this response does not have a distinguished role. However, this is an important parameter to predict the stability of colloidal dispersions, and so it should always be measured and analyzed. Hence, particle size will be the main response evaluated on further experimental designs. Zeta potential will be estimated as a complement for nanoparticle characterization, and to verify the agreement with size results.

6.5. DESIGN 3

The preliminary results obtain from the previous designs, allowed us to predict the nanoparticle behavior according to the different components tested, thus establishing the factors and interactions that determine the response. NLC-PO formulation, produced with Tween® 80 contrasts with the other ones, allowing to obtain smaller and stable particles. Oleic acid appears to be a promising lipid to work with, since the pronounced influence of the variables selected enables some experimentation towards the formulation optimization. Moreover, the results analyzed above also presented the favorable interactions for this system, leading to smaller particles, and supporting the initial measurements performed. The full factorial 2^k designs applied enabled the choice of the greatest components for the formulation to be optimized. The NLC formulation studied on this experimental design was composed by Precirol® ATO 5, oleic acid and Tween® 80.

The third experimental design performed was a central composite design (circumscribed) consisting of a three-factor, two-level design, plus six star points on the axes and replicated points at the center of the design. The response defined was particle size, *D*, but zeta potential was also measured for nanoparticle characterization and to assess the agreement with particle size results. The Tween® 80 concentration (x_1), liquid:solid lipid ratio (x_2), and lipid concentration (x_3) were the independent variables selected. Each independent variable was coded with -1 and +1 levels. Table 21 summaries the conditions investigated, and Table 22 gathers the particle properties measured for the conditions referred.

Table 21. Conditions investigated in the central composite design performed.

	- α	**-1**	**Center point**	**+1**	**+ α**
Tween® 80 Concentration %(w/v) x_1	1%	2%	3.5%	5%	6%
Liquid:solid lipid ratio (w/w) x_2	0:100	10:90	25:75	40:60	50:50
Lipid Concentration %(w/w) x_3	2%	3%	4.5%	6%	7%

The results obtained support some conclusions taken from the previous experimental designs. It is clearly visible that an increase on the liquid:solid lipid ratio reduces particle size, evidencing the effect of the presence of a liquid lipid in the system composition.

Table 22. Particle size, polydispersity index (PI) and zeta potential values obtained for the conditions defined above. Values represented as mean ± SD (*n*=3).

Liquid:solid lipid ratio (w/w)	Lipid Concentration %(w/w)	Tween® 80 Concentration %(w/v)	Particle size (nm)	PI	Zeta potential (mV)
0:100	4.5%	3.5%	534 ± 6	0.271 ± 0.005	-16.9 ± 0.9
10:90	3%	2%	254 ± 4	0.294 ± 0.010	-29.3 ± 0.8
		5%	244 ± 7	0.29 ± 0.02	-38.5 ± 1.4
	6%	2%	395 ± 19	0.268 ± 0.016	-34.5 ± 0.9
		5%	334 ± 6	0.20 ± 0.03	-22.8 ± 0.5
25:75	2%	3.5%	226 ± 11	0.31 ± 0.02	-24.6 ± 1.4
	4.5%	1%	348 ± 16	0.27 ± 0.04	-25.87 ± 0.05
		3.5%	183 ± 5	0.291 ± 0.017	-28.9 ± 0.9
		6%	177.4 ± 0.3	0.324 ± 0.003	-25.7 ± 0.7
	7%	3.5%	280 ± 8	0.273 ± 0.007	-23.4 ± 1.1
40:60	3%	2%	151 ± 2	0.269 ± 0.012	-26 ± 3
		5%	105.4 ± 0.6	0.311 ± 0.010	-32 ± 3
	6%	2%	291 ± 23	0.23 ± 0.05	-29.1 ± 0.9
		5%	232 ± 26	0.20 ± 0.04	-31.9± 0.9
50:50	4.5%	3.5%	124 ± 3	0.271 ± 0.009	-28.1 ± 0.6

In general, Tween® 80 provided good stability for these formulations. The larger ionization at the interface tends to increase electrostatic repulsion, preventing aggregation. Moreover, Tween® 80 molecules attached to the particle surface provide steric stability.

With these experimental data, the model coefficients were estimated by least squares linear regression, and the results are presented on the Table 23.

The full second-order model obtained consists of 11 terms. In a first analysis, the conclusions are very similar to the ones obtained from preceding designs. An increase in Tween® 80 concentration will decrease particle size, and an increase in the lipid concentration will increase it.

Table 23. Parameters obtained from the central composite design in the indicated conditions and Student's *t*-test analysis.

Response term	Particle size	*t*-value	Level of confidence	Zeta potential	*t*-value	Level of confidence
β_0	182.73	6.34	100.00	-28.94	-11.88	100.00
β_1	-33.71	-4.38	99.99	-0.58	-0.89	62.28
β_2	-82.80	-10.76	100.00	-1.17	-1.80	91.89
β_3	42.05	5.46	100.00	0.50	0.76	55.01
β_{12}	-4.16	-0.41	31.47	-0.98	-1.14	73.87
β_{23}	4.42	0.43	33.31	-1.30	-1.51	85.85
β_{13}	-7.80	-0.77	55.13	3.30	3.83	99.95
β_{11}	20.82	1.83	92.39	-0.10	-0.11	8.59
β_{22}	42.98	3.78	99.94	0.97	1.01	68.02
β_{33}	17.51	1.54	86.69	0.50	0.52	39.30
β_{123}	4.61	0.45	34.65	-2.64	-3.07	99.58

The most important parameter was the liquid:solid lipid ratio, followed by Tween® 80 concentration, as seen by the high magnitude of the respective coefficients obtained for both responses. The third variable had a positive coefficient, showing that a higher lipid concentration lead to larger particle size, as previously observed. The evaluation of the interactions was focused only on paired analysis (β_{12}, β_{23} and β_{13}). However, these are not large, and the respective influence is considered small. Moreover, they were not statistical significant. The interpretation of β_{123} interaction is more complex, and since it was not statistical significant, this was not discussed. The quadratic interactions will be analyzed below.

Focusing now on zeta potential as response of the system, the influence of the variables followed the same trend observed for particle size, as revealed by the magnitude of the coefficients. Again, the most important parameter was the liquid:solid lipid ratio, followed by the emulsifier concentration and lipid concentration. An increase in the liquid:solid lipid ratio, and in the emulsifier concentration yield a more negative zeta values, thus indicating more stable systems. Conversely, an increase in the lipid concentration rendered less stability upon the system. However, the majority of the coefficients do not have statistical

significance, probably due to low discrepancy among the values obtained. Hence, optimization was mainly carried out based on particle size, using zeta potential as complement for the characterization of the optimized formulation (see Table 24).

In order to proceed with the optimization process, the current model can be graphically represented by a parabola (or paraboloid), wherein the magnitude of the quadratic terms control the curvature of the response surface. The high magnitude of these coefficients is comparable to the magnitude of the main effects coefficients β_1, β_2 and β_3. Both are elevated, thus confirming the pronounced influence of these on the system response. Moreover, when these are positive, the parabola passes through a minimum and when they are negative, it passes through a maximum (ARMSTRONG, 2006). Thus, the positive sign of the quadratic terms found indicated a minimum stationary point. To calculate the position of this value, derivatives of the model equation were calculated and equated to zero. The system was solved and the coded values converted to real values. Moreover, by applying the optimized model, it was possible to predict the characteristics of the optimal formulation, such as particle size and zeta potential. Table 24 presents the optimal values for the factors under study.

Table 24. Coded values and real values for particle size and zeta potential for each factor studied. Experimental values represented as mean ± SD (*n*=9).

		Coded value	Real value	Predicted value	Experimental value
Particle size	Tween® 80 Concentration %(w/v) x_1	0,69	4,54		
	Liquid:solid lipid ratio x_2	1,06	40,86	102.45	134 ± 26
	Lipid Concentration %(w/w) x_3	-1,18	2,73		
Zeta potential	Tween® 80 Concentration %(w/v) x_1	0.08	3,63		
	Liquid:solid lipid ratio x_2	0.96	39.34	-29.41	-35 ± 2
	Lipid Concentration %(w/w) x_3	0.47	5.20		

The estimated values extracted from the model are in good agreement with the experimental results, reinforcing the role of the factorial planning for the optimization procedure. It should be noted that this formulation combines not only a low particle size but also a suitable stability.

For the rationalization of the optimized system, response-surface methodology was applied. For that, one of the factors was set to the optimal value, and the behavior of the remaining analyzed. The response surfaces obtained are exhibited in Figures 10-12.

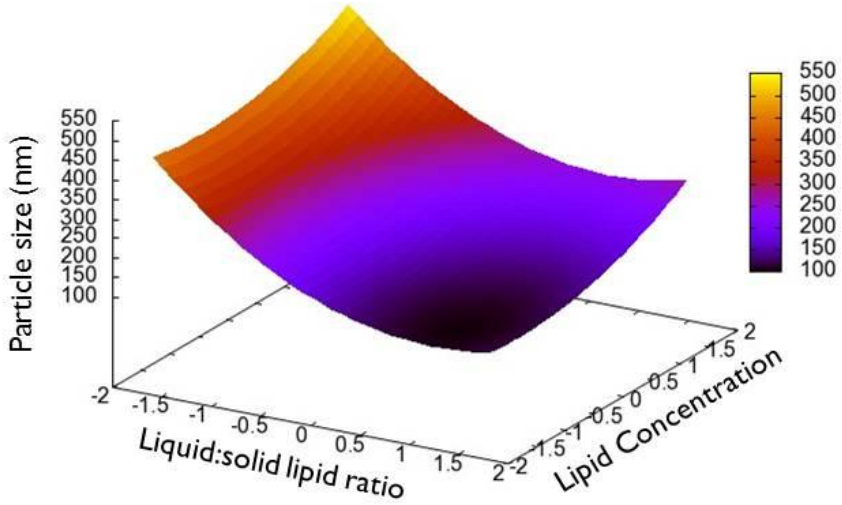

Figure 10. Particle size response surface for the optimal Tween® 80 concentration.

The influence of the variables is clearly depicted by the curvature and color change on the surface plot.

Keeping constant the optimal Tween® 80 concentration, a decrease in particle size is promoted by a lower lipid concentration and a higher liquid:solid lipid ratio (Figure 10). The size reduction prompted by a higher liquid:solid lipid ratio is clearly evident when comparing with the SLN initially prepared. This could be attributed to a lower viscosity of the dispersed phase (MEHNERT and MÄDER, 2001). Additionally, it is described that the particle size is increased with higher melting point lipids. The liquid:solid lipid ratio affects, to a large degree, the particle size obtained (VITORINO *et al.*, 2013). The same applies when a lower lipid concentration is present.

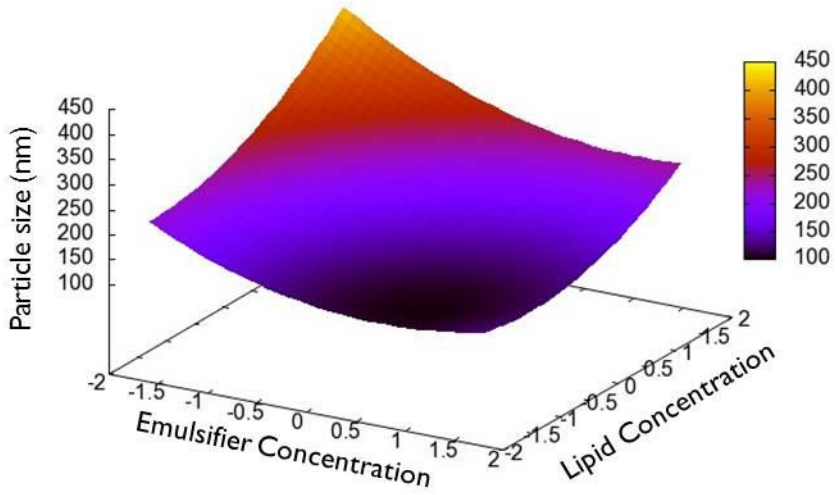

Figure 11. Particle size response surface for the optimal liquid:solid lipid ratio.

Figure 11 indicates that the optimal size range is obtained for a high emulsifier and low lipid concentration, as clearly illustrated by the black area of the plot. Considering the optimal liquid:solid lipid ratio, a lower lipid concentration and higher emulsifier concentration will reduce particle size. This behavior corroborates the coefficient values previously obtained (Table 23).

A rational for that has already been described in the literature (MEHNERT and MÄDER, 2001). Higher emulsifier concentrations reduce the surface tension and facilitate particle partition during homogenization, leading to an increase in surface area, which is associated to a decrease in size. It has also been shown that an increase in lipid content results in larger particles and broader size distributions, which could be ascribed to a decrease in the homogenization efficiency and an increase in particle agglomeration (MEHNERT and MÄDER, 2001; MÜLLER, RADTKE, and WISSING, 2002).

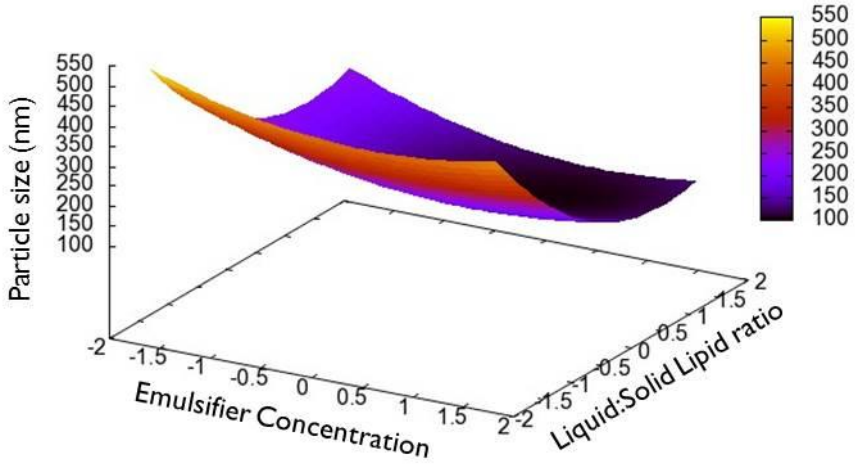

Figure 12. Particle size response surface for the optimal lipid concentration.

A detailed analysis of Figure 12 validates several trends previously identified. Note that for a lower liquid:solid lipid ratio, the effect of the emulsifier concentration is not significantly visible, and the particles obtained will be larger. Again, this could be attributed to a high viscosity of the inner phase, which will condition the effect in size reduction promoted by an increase in the emulsifier concentration from –α to +α level. This was also perceived throughout the previous analyses carried out.

The prediction performed with the optimal model was thus sequentially confirmed and rationalized, providing an useful platform for the optimization process.

CHAPTER 7

PORPHYRIN INCORPORATION ON THE OPTIMAL FORMULATION

As an example of application of the optimal formulation achieved, three porphyrins, with different molecular structures, were screened for incorporation on NLC. The porphyrin solubility in the liquid (Table 26) and solid lipids was determined through fluorimetry. In general, porphyrin solubility in the solid liquid was below 2.66 ± 0.64 μg/mL. The higher solubility was obtained for TPP, which is in accordance with the lack of polar groups in the structure. Since solubility of the drug in the melted lipid is an important parameter for acceptable entrapment efficiency (VITORINO *et al.*, 2013), the porphyrin with higher solubility in oleic acid (TPP) was selected for NLC incorporation.

Table 25. Values for porphyrin solubility (μg/mL) on the liquids investigated. Results are expressed as mean ± SD (*n*=3).

Porphyrin Solubility	**TPP**	**MP-1046**	**BFON-60**
Oleic Acid	1125 ± 235	242 ± 26	398 ± 49

TPP was then encapsulated on the optimized formulation, in order to assess its influence on the formulation properties, such as particle size and zeta potential.

7.1. Characterization of Drug-Loaded NLC

The characterization of the formulation after drug incorporation is an important tool to assess the properties of the system developed. As described before, particle size and zeta potential measurements were performed by PCS (Table 27).

Table 26. Particle size and zeta potential measurements (mean ± SD (*n*=9)) of the optimal formulation before and after porphyrin incorporation.

Parameters	**Unloaded NLC**	**TPP NLC**
Particle Size (nm)	134 ± 26	121 ± 18
Polydispersity Index	0.307 ± 0.014	0.302 ± 0.007
Zeta Potential (mV)	-35 ± 2	-35.5 ± 1.6

According to these results, the porphyrin incorporation slightly reduces particle size. The dispersion remains stable, and the size distribution was not considerably altered.

LD was also performed to confirm the absence of microparticles in the optimized formulation (Table 28).

Table 27. Span value determined by laser diffractometry.

Formulation	Span Value
Unloaded NLC	94.856
NLC TPP	34.485

The LD measurements indicate the existence of a small population of microparticles in the dispersion. The porphyrin incorporation lead to a reduction in the broadness of size distribution, as indicated by the lower span value obtained (Table 28). These results are coherent with the analysis performed by PCS.

To confirm the particle size and morphology, a SEM analysis was also conducted (Figure 13).

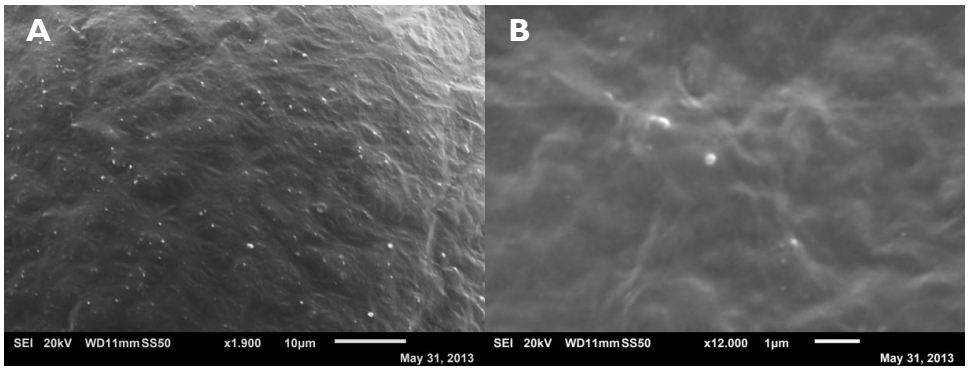

Figure 13. SEM images from the optimized formulation after porphyrin incorporation. (A) 10 µm scale and (B) 1 µm scale.

The image on the left (A) showed an homogenous size distribution, in accordance to the PI values. The particle size typically not exceeding 1 µm is also confirmed, as observed in particular on panel (B).

The drug incorporation did not promote major alterations on the particle properties, which suggests this optimized formulation is promissing for incorporation of this porphyrin.

7.2. Entrapment Efficiency

As mentioned before, a major problem to overcome in PDT is drug delivery. In this field, nanoparticles can increase the solubility of hydrophobic drugs, and due to their small size

enable the accumulation in tumor tissue, thus reducing damage to healthy tissue. It was shown that the porphyrin incorporation on the optimized formulation did not change the particle properties. It is also important to assess the proper incorporation of the drug by quantifying the EE value.

As mentioned in Chapter 5, EE was calculated indirectly by measuring the concentration of the free drug in the aqueous phase after nanoparticles separation by ultrafiltration-centrifugation. The EE determination revealed itself as a difficult task.

Firstly, the total amount of porphyrin in the dispersion was determined. Although the method for porphyrin quantification by fluorimetry was validated, the relation between the fluorescence and the area is not linear for the range of concentrations used. The area under the fluorescence spectra presented a linear relation with the concentration between 0.066 and 0.011 μg/mL. An increase in concentration up to 0.164 μg/mL also showed a linear relation, but the interference of physical phenomenon as dispersion and photophysical processes, such as auto-quenching, lead to a different slope in the linear correlation. Thus, different calibration curves were used, according to the concentrations obtained in the assays. However, the results obtained were clearly excessive and fluctuating, not allowing the correct determination of the total amount of porphyrin in the dispersion. Although there are different hypotheses to justify the obtained values, the decision was to consider that the total amount of porphyrin in the dispersion was equal to the amount of porphyrin added when the NLC were produced, excluding possible drug losses during the process, or experimental errors. The EE, determined according to equation presented on 5.11, was 92 ± 6%. The high EE obtained is in accordance with the expected values, since NLC enables a high drug loading due to their highly disordered matrix with many imperfections to accommodate the drug.

Further work is necessary to ensure a correct and precise EE determination. There is current work for developing a method for this quantification. High-performance liquid chromatography is being assessed as an alternative to EE determination.

Chapter 8
Concluding Remarks

Drug delivery is one of the main challenges to be overcome in PDT. An effective carrier should promote selective accumulation of the PS in tumor tissue in therapeutic concentrations, with reduced or no uptake from non-target cells. Nanoparticles have great interest as drug carriers. In particularly, lipid nanoparticles, such as SLN and NLC, have been studied for various administration routes. Both these systems have several advantages such as the ability to protect the drug from degradation, good physical stability and controlled drug release. Additionally, NLC enable a high pay-load and prevent drug expulsion due to their nanostructure. Despite their advantages, these have not been extensively studied for application in PDT. The present investigation allowed the assessment of its potential as PS carriers. Firstly, to define the formulation composition, several experimental designs were performed in order to achieve an optimal formulation.

The process of evaluating and characterizing a system, identifying major factors and how the response is influenced by them, is of great importance. It enables a reduction of the number of experiments, and the evaluation of relevance and statistical significance of the factors studied as well as the interaction between them through the development of mathematical models. Particularly, in the pharmaceutical field where the resources available should be managed with care and good results must be achieved, the application of experimental design is essential to the project success.

In this work, experimental design proved to be highly useful in the optimization process. SLN and NLC compositions were studied in order to evaluate the influence of different parameters, such as emulsifier concentration, lipid concentration, the liquid:solid lipid ratio and the absence or presence of a liquid lipid, on particle size and zeta potential of the dispersion obtained. The system selected for optimization consisted of NLC. Several experimental designs were applied, and the optimal formulation achieved was composed by Precirol® ATO 5, oleic acid and Tween® 80, with a liquid:solid lipid ratio of 40.86:59.14 (w/w), a lipid concentration of 2.73% (w/w) and an emulsifier concentration of 4.54% (w/v). As described in the literature, the influence of a higher emulsifier concentration and lower lipid concentration on size reduction was confirmed. Moreover, it is clearly revealed the crucial role of the liquid:solid lipid ratio on size reduction of NLC.

Additionally, NLC produced were evaluated for porphyrin incorporation to confirm its potential as PS carriers. The loaded-NLC maintained their small size, stability and narrow size distribution. The main obstacle during this work was the determination of EE, which was

not successfully completed. Despite the fact that it was not possible to measure the exact amount of porphyrin incorporated on NLC, incorporation it was clear, thus confirming the potential of the optimized system.

In conclusion, this work provided important information for the application of NLC on PDT. The appropriate size and stability was achieved for this system and, through the application of experimental design, it was possible to effectively achieve a formulation with the desired optimal properties. This can be selected as promising carrier for TPP.

However, this subject requires further investigation. These systems have had little study for this specific application, and additional characterization is needed. Other techniques would include laser diffractometry (LD) to confirm the presence of larger particles in the dispersion, atomic force microscopy (AFM) and transmission electron microscopy (TEM), to obtain detailed information on morphology, size and surface properties of NLC, and attenuated total reflectance infrared spectroscopy (ATR-FTIR) for more detailed information about the structure of the particles. To investigate the status of the lipids differential scanning calorimetry (DSC) should be applied. Nuclear magnetic resonance (NMR) and electron spin resonance (ESR) are sensitive methods which can be employed for the detection of the presence of different colloidal species that can be formed during the production process of SLN and NLC aqueous dispersions. Stability studies to assess the physicochemical stability for a long period are also important. In vitro and in vivo studies for the performance assessment of the optimized system are also necessary.

The parenteral delivery is the most challenging area in drug delivery. However, lipid nanoparticles provide some advantages, such as controlled release of the drug, high drug loading capacity and enhanced bioavailability. Several active compounds have been studied for incorporation on NLC, and some have proven their efficacy. In this work we provided an additional understanding on NLC and its future application in this field.

REFERENCE LIST

ARMSTRONG, N.A. - Pharmaceutical Experimental Design and Interpretation. 2th edition. New York: Taylor & Francis Group, 2006. ISBN 0-415-29901-2.

BECHET, D. *ET AL.* - Nanoparticles as vehicles for delivery of photodynamic therapy agents. Trends in Biotechnology. Vol 26, 11 (2008), 612–621.

BONNETT, R. - Chemical Aspects of Photodynamic Therapy. 1st edition. London: Gordon and breach Science Publishers, 2000. ISBN 90-5699-248-1.

BOVIS, M.J. *ET AL.* - Improved *in vivo* delivery of m-THPC via pegylated liposomes for use in photodynamic therapy. Journal of Controlled Release. Vol 157, 2 (2012), 196–205.

BUNJES, H. - Lipid nanoparticles for the delivery of poorly water-soluble drugs. The Journal of Pharmacy and Pharmacology. Vol 62, 11 (2010), 1637–1645.

CHATTERJEE, D.K., FONG, L.S. AND ZHANG, Y. - Nanoparticles in photodynamic therapy: an emerging paradigm. Advanced Drug Delivery Reviews. Vol 60, 15 (2008), 1627–1637.

CHEN, B., POGUE, B.W. AND HASAN, T. - Liposomal delivery of photosensitising agents. Expert Opinion on Drug Delivery. Vol 2, 3 (2005), 477–487.

COMPANY, W.G. - High-Quality Ingredients for Personal Care and Pharmaceutical Applications. [Accessed 25 June 2013]. Available in: http://www.warnergraham.com/products/olefins-surfactants-emollients/cremer-oleo/.

DABROWSKI, J.M. *ET AL.* - Synthesis, photophysical studies and anticancer activity of a new halogenated water-soluble porphyrin. Photochemistry and Photobiology. Vol 83, 4 (2007), 897–903.

DEROSA, M.C. AND CRUTCHLEY, R.J. - Photosensitized singlet oxygen and its applications. Coordination Chemistry Reviews. Vol 233-234, (2002), 351–371.

DOKTOROVOVA, S. AND SOUTO, E.B. - Nanostructured lipid carrier-based hydrogel formulations for drug delivery: a comprehensive review. Expert Opinion on Drug Delivery. Vol 6, 2 (2009), 165–176.

DOLMANS, D.E.J.G. - Photodynamic therapy for cancer. Nature Reviews Cancer. Vol 3, (2003), 375–380.

DOUGHERTY, T.J. *ET AL.* - Photoradiation therapy. II. Cure of animal tumors with hematoporphyrin and light. Journal of the National Cancer Institute. Vol 55, 1 (1975), 115–121.

DOUGHERTY, T.J. *ET AL.* - Photoradiation Therapy for the Treatment of Malignant Tumors. Cancer Research, Vol 38 (1978), 2628–2635.

EATON, J.W. - GNU Octave Software, version 3.2.3, 2009.

FANG, J.Y. ET AL. - Lipid nanoparticles as vehicles for topical psoralen delivery: solid lipid nanoparticles (SLN) versus nanostructured lipid carriers (NLC). European Journal of Pharmaceutics and Biopharmaceutics. Vol 70, 2 (2008), 633–640.

FERREIRA, S.L.C. *ET AL.*. - Box-Behnken design: An alternative for the optimization of analytical methods. Analytica Chimica Acta. Vol 597, 2 (2007), 179–186.

HOPPER, C. - Photodynamic therapy: a clinical reality in the treatment of cancer. The Lancet Oncology. Vol 1, (2000), 212–219.

HUANG, Z. *ET AL.* - Development and evaluation of lipid nanoparticles for camptothecin delivery: a comparison of solid lipid nanoparticles, nanostructured lipid carriers, and lipid emulsion. Acta Pharmacologica Sinica. Vol 29, 9 (2008), 1094–1102.

IQBAL, M.A. *ET AL.* - Nanostructured lipid carriers system: recent advances in drug delivery. Journal of Drug Targeting. Vol 20, 10 (2012), 813–830.

JOHNSTONE, R.A.W. *ET AL.* - Improved Syntheses of 5,10,15,20-Tetrakisaryl- and Tetrakisalkylporphyrins. Heterocycles. Vol 43, 7 (1996), 1423–1437.

JOSHI, M. AND PATRAVALE, V. - Nanostructured lipid carrier (NLC) based gel of celecoxib. International Journal of Pharmaceutics. Vol 346, 1–2 (2008), 124–132.

JOSHI, M.D. AND MÜLLER, R.H. - Lipid nanoparticles for parenteral delivery of actives. European Journal of Pharmaceutics and Biopharmaceutics. Vol 71, 2 (2009), 161–172.

KONAN, Y.N., CERNY, R., *ET AL.* - Preparation and characterization of sterile sub-200 nm for photodynamic therapy. European Journal of Pharmaceutical Sciences. Vol 55, (2003), 115–124.

KONAN, Y.N., BERTON, M., *ET AL.* - Enhanced photodynamic activity of meso-tetra(4-hydroxyphenyl)porphyrin by incorporation into sub-200 nm nanoparticles. European Journal of Pharmaceutical Sciences. Vol 18, 3–4 (2003), 241–249.

KONAN, Y.N., GURNY, R. AND ALLÉMANN, E. - State of the art in the delivery of photosensitizers for photodynamic therapy. Journal of Photochemistry and Photobiology: B: Biology. Vol 66, 2 (2002), 89–106.

LEWIS, G.A., MATHIEU, D. AND PHAN-TAN-LUU, R. - Pharmaceutical Experimental Design. 1st. Marcel Dekker: New York, 1999. ISBN 0-8247-9860-0

LIM, C.-K. *ET AL.* - Nanophotosensitizers toward advanced photodynamic therapy of Cancer. Cancer Letters. (2012). http://dx.doi.org/10.1016/j.canlet.2012.09.012

LIPSON, R.L. AND BALDES, E.J. - The Photodynamic Properties of a Particular Hematoporphyrin Derivative. Archives of Dermatology. Vol 82, 4 (1960), 508–516.

LIPSON, R.L., BALDES, E.J. AND OLSEN, A.M. - The Use of a Derivative of Hematoporphyrin in Tumor Detection. Journal of the National Cancer Institute. Vol 26, (1961), 1–11.

LIU, D. *ET AL.* - Nanostructured lipid carriers as novel carrier for parenteral delivery of docetaxel. Colloids and Surfaces B: Biointerfaces. Vol 85, 2 (2011), 262–269.

LUKŠIENE, Ž. - Photodynamic therapy: mechanism of action and ways to improve the efficiency of treatment. Medicina. Vol 39, 12 (2003).

MEHNERT, W. AND MÄDER, K. - Solid lipid nanoparticles: Production, characterization and applications. Advanced Drug Delivery Reviews. Vol 47, 2–3 (2001), 165–196.

MUCHOW, M. *ET AL.* - Production and characterization of testosterone undecanoate-loaded NLC for oral bioavailability enhancement. Drug Development and Industrial Pharmacy. Vol 37, 1 (2011), 8–14.

MÜLLER, R.H. *ET AL.* - Nanostructured lipid carriers (NLC) in cosmetic dermal products. Advanced Drug Delivery Reviews. Vol 59, 6 (2007), 522–530.

MÜLLER, R.H., MÄDER, K. AND GOHLA, S. - Solid lipid nanoparticles (SLN) for controlled drug delivery - a review of the state of the art. European Journal of Pharmaceutics and Biopharmaceutics. Vol 50, 1 (2000), 161–177.

MÜLLER, R.H., RADTKE, M. AND WISSING, S.A. - Solid lipid nanoparticles (SLN) and nanostructured lipid carriers (NLC) in cosmetic and dermatological preparations. Advanced Drug Delivery Reviews. Vol 54, 1 (2002), S131–55.

MÜLLER, R.H., SHEGOKAR, R. AND KECK, C.M. - 20 years of lipid nanoparticles (SLN and NLC): present state of development and industrial applications. Current Drug Discovery Technologies. Vol 8, 3 (2011), 207–227.

NASCIMENTO, B.F.O., ROCHA GONÇALVES, A.M. AND PINEIRO, M. - MnO_2 instead of quinones as selective oxidant of tetrapyrrolic macrocycles. Inorganic Chemistry Communications. Vol 13, 3 (2010), 395–398.

PAIS, A.A.C.C. - Experimental Design. In Catalysis from Theory to Application Coimbra, Imprensa da Universidade de Coimbra. 978-989-8074-35-5, 567–584.

PARDEIKE, J., HOMMOSS, A. AND MÜLLER, R.H. - Lipid nanoparticles (SLN, NLC) in cosmetic and pharmaceutical dermal products. International Journal of Pharmaceutics. Vol 366, 1–2 (2009), 170–184.

PARDEIKE, J. AND MÜLLER, R.H. - Coenzyme Q10 loaded NLCs: preparation, occlusion properties and penetration enhancement. Pharmaceutical Technology Europe. Vol 19, (2007), 46–49.

PASZKO, E. *ET AL.* - Nanodrug applications in photodynamic therapy. Photodiagnosis and Photodynamic Therapy. Vol 8, 1 (2011), 14–29.

PINNACLE - Label Information approved on 24/06/2011 for Photofrin®, NDA no 020451. Available in: http://www.accessdata.fda.gov/scripts/cder/drugsatfda/index.cfm?fuseaction=Search.Label_ApprovalHistory.

PUGLIA, C. AND BONINA, F. - Lipid nanoparticles as novel delivery systems for cosmetics and dermal pharmaceuticals. Expert Opinion on Drug Delivery. Vol 9, 4 (2012), 429–441.

ROWE, R.C., SHESKEY, P.J. AND OWEN, S.C. - Handbook of Pharmaceutical Excipients. 5th edition. London: Pharmaceutical Press and American Pharmacists Association, 2006. ISBN 0-85369-618-7

ROY, I. *ET AL.* - Ceramic-based nanoparticles entrapping water-insoluble photosensitizing anticancer drugs: a novel drug-carrier system for photodynamic therapy. Journal of American Chemical Society. Vol 125, 26 (2003), 7860–7865.

SERRA, A. *ET AL.* - A look at clinical applications and developments of photodynamic therapy. Oncology Reviews. 2 (2008), 189–203.

SOUTO, E.M.B. - SLN and NLC as Drug Carriers of Clotrimazole for Hydrogel Topical Formulations. Faculty of Pharmacy, University of Porto. 2003.

STEVENS, P.J., SEKIDO, M. AND LEE, R.J. - Synthesis and evaluation of a hematoporphyrin derivative in a folate receptor-targeted solid-lipid nanoparticle formulation. Anticancer Research. Vol 24, 1 (2004), 161–165.

TEERANACHAIDEEKUL, V. *ET AL.* - Cetyl palmitate-based NLC for topical delivery of Coenzyme Q10 - development, physicochemical characterization and in vitro release studies. European Journal of Pharmaceutics and Biopharmaceutics. Vol 67, 1 (2007), 141–148.

TORCHILIN, V.P. - Targeted pharmaceutical nanocarriers for cancer therapy and imaging. The American Association of Pharmaceutical Scientists Journal. Vol 9, 2 (2007), E128–47.

TRIESSCHEIJN, M. *ET AL.* - Photodynamic therapy in oncology. The Oncologist. Vol 11, 9 (2006), 1034–1044.

UNER, M. AND YENER, G. - Importance of solid lipid nanoparticles (SLN) in various administration routes and future perspectives. International Journal of Nanomedicine. Vol 2, 3 (2007), 289–300.

VITORINO, C. *ET AL.* - The size of solid lipid nanoparticles: an interpretation from experimental design. Colloids and Surfaces B: Biointerfaces. Vol 84, 1 (2011), 117–130.

VITORINO, C. *ET AL.* - Co-encapsulating nanostructured lipid carriers for transdermal application: from experimental design to the molecular detail. Journal of Controlled Release. Vol 167, 3 (2013), 301–314.

WIEDER, M.E. *ET AL.* - Intracellular photodynamic therapy with photosensitizer-nanoparticle conjugates: cancer therapy using a "Trojan horse". Photochemical & Photobiological Sciences. Vol 5, 8 (2006), 727–734.

WILKINSON, F., HELMAN, P.W. AND ROSS, A.B. - Quantum Yield for the Photosensitized Formation of the Lowest Electronically Excited Singlet State of Molecular Oxygen in Solution. Journal of Physical and Chemical Reference Data. Vol 22, 1 (1993).

WISSING, S.A., KAYSER, O. AND MÜLLER, R.H. - Solid lipid nanoparticles for parenteral drug delivery. Advanced Drug Delivery Reviews. Vol 56, 9 (2004), 1257–1272.

WOITISKI, C.B. *ET AL.* - Design for optimization of nanoparticles integrating biomaterials for orally dosed insulin. European Journal of Pharmaceutics and Biopharmaceutics. Vol 73, 1 (2009), 25–33.

ZHANG, J., FAN, Y. AND SMITH, E. - Experimental Design for the Optimization of Lipid Nanoparticles. Pharmaceutical Nanotechnology. Vol 98, 5 (2009), 1813–1819.